SIDE LOBE SUPRESSION TECHNIQUES FOR POLYPHASE CODES IN RADAR

A THESIS SUBMITTED IN PARTIAL FULFILLMENT

OF THE REQUIRMENT FOR THE DEGREE OF

Master of Technology

In

Telematics and Signal Processing

By

VIJAY RAMYA KOLLI

209EC1108

DEPARTMENT OF ELECTRONICS AND COMMUNICATION ENGINEERING
NATIONAL INSTITUTE OF TECHNOLOGY
ROURKELA, INDIA
2011

SIDE LOBE SUPRESSION TECHNIQUES FOR POLYPHASE CODES IN RADAR

A THESIS SUBMITTED IN PARTIAL FULFILLMENT

OF THE REQUIRMENT FOR THE DEGREE OF

Master of Technology

In

Telematics and Signal Processing

By

VIJAY RAMYA KOLLI

209EC1108

Under guidance of

Prof. AJIT KUMAR SAHOO

DEPARTMENT OF ELECTRONICS AND COMMUNICATION ENGINEERING
NATIONAL INSTITUTE OF TECHNOLOGY
ROURKELA, INDIA
2011

NATIONAL INSTITUTE OF TECHNOLOGY

ROURKELA

CERTIFICATE

This is to certify that the thesis report entitled "**SIDE LOBE SUPRESSION TECHNIQUES FOR POLYPHASE CODES IN RADAR"**submitted by **Ms VIJAY RAMYA KOLLI**, **Roll No: 209EC1108**, in partial fulfillment of the requirements for the award of Master of Technology degree in Electronics and Communication Engineering Department with specialization in "Telematics and Signal Processing" at the National Institute of Technology, Rourkela and is an authentic work carried out by her under my supervision and guidance.

To the best of my knowledge, the matter embodied in the thesis has not been submitted to any other University / Institute for the award of any Degree or Diploma.

Place**:** NIT Rourkela

Date:

Prof. Ajit kumar Sahoo

(Supervisor)

Dept. of Electronics & Communication Engg.

National Institute of Technology,

Rourkela - 769008.

Acknowledgment

I am deeply indebted to Prof**. Ajit Kumar Sahoo,** my supervisor and the guiding force behind this project. I want to thank him for introducing me to the field of Signal Processing and giving me the opportunity to work under him. In spite of his extremely busy schedules in Department, he was always available to share with me his deep insights, wide knowledge and extensive experience. His advices have value lasting much beyond this project. I consider it a blessing to be associated with him.

I express my respects to **Prof**. **S.K. Patra**, **Prof**. **K.K. Mahapatra**, **Prof**. **G. S. Rath**, **Prof**. **S. Meher**, **Prof**. **Poonam Singh**, **Prof**. **D.P.Acharya**, **Prof**. **Samit Ari**, and **Prof. NVLN.Murthy,** for teaching me and also helping me how to learn. And also I would like to thanks all faculty members of ECE Department for their generous help in various ways for the completion of this thesis. They have been great sources of inspiration to me and I thank them from the bottom of my heart.

I am very thankful to my friend **Lakshman kumar**, who helped me a lot during my research work. I would also like to thank all my friends and especially my classmates for all the thoughtful and mind stimulating discussions we had, which prompted us to think beyond the obvious. Last but not least I would like to thank my parents. They are my first teachers when I came into this world, who taught me the value of hard work by their own example. They rendered me enormous support being apart during the whole tenure of my stay in NIT Rourkela

VIJAYRAMYA

ABSTRACT

The present thesis aims to make an in-depth study of Radar pulse compression. Pulse compression (PC) is an important module in many of the modern radar systems. It is used to overcome major problem of a radar system that requires a long pulse to achieve large radiated energy but simultaneously a short pulse for range resolution .Range resolution is an ability of the receiver to detect nearby targets. The performance measures of PC techniques are PSL, ISL, SNR loss and Doppler shift. The major advantages of PC are resulting gain in SNR and relative tolerance to jammers. PC can also lift small target signals out of clutter.

In this thesis we compare the merit factors of different sidelobe reduction techniques with a novel technique, using P4 code of length 1000. The amplitude weighting technique in which the code signal is multiplied with the window coefficients and the weighted code and the transmitted signal are applied to correlation in the receiver side .The tradeoff in reducing the PSL is spreading of the compressed pulse. Woo filter technique is that which uses two correlation filters to produce a single discrete filter, It reduces PSL and ISL at sacrifice of mainlobe splitting and 3 [dB] SNR loss. The modified forms of Woo filter reduce the PSL further and also the mainlobe splitting present in Woo filter is removed. Asymmetrical weighting is a technique in which amplitude of the Woo filter is taken as the weighting function to the incoming signal. This method enables to suppress PSL beyond Barker codes levels while other performance degradations are minimized.

In the proposed technique amplitude weighting is applied to a combination of the incoming signal and one-bit shifted version of the incoming signal. This technique produces better peak side lobe ratio (PSL) and integrated side lobe ratio (ISL) than all other conventional sidelobe reduction techniques. Main lobe splitting which is the main disadvantage in Woo filter is eliminated in this techniques and it is easy to implement and incurs a minimal signal to noise ratio SNR loss.

Keywords

Radar Pulse Compression, PSL.ISL, SNR.

CONTENTS

Chapter- 3 Conventional Sidelobe Reduction techniques for polyphase codes

Chapter-4 WOO Filter sidelobe reduction technique for pulse compression.

Chapter-5 Conclusion and scope for future work

LIST OF FIGURES

LIST OF TABLES

Chapter 1

Introduction

1.1. Background

RADAR is an acronym of Radio Detection And Ranging. It is an object-detection system which uses electromagnetic waves specifically radio waves to determine the range, altitude, direction or speed of both moving and fixed objects such as aircraft ,ships, spacecraft ,guided missiles ,motor vehicles, weather formations, and terrain. The radar dish, or antenna, transmits pulses of radio waves or microwaves which bounce off any object in their path. The object returns a tiny part of the wave's energy to a dish or antenna which is usually located at the same site as the transmitter. The modern uses of radar are highly diverse, including air traffic control, radar astronomy, and aircraft anti-collision systems, antimissile. [1.1, 1.2].

The rapid advances in digital technology made many theoretical capabilities practical with digital signal processing and digital data processing. Radar signal processing is defined as the manipulation of the received signal, represented in digital format, to extract the desired information whilst rejecting unwanted signals. Pulse compression allowed the use of long waveforms to obtain high energy simultaneously achieves the resolution of a short pulse by internal modulation of the long pulse. The resolution is the ability of radar to distinguish targets that are closely spaced together in either range or bearing. The internal modulation may be binary phase coding, polyphase coding, frequency modulation, and frequency stepping. There are many advantages of using pulse compression techniques in the radar field. They include reduction of peak power, relevant reduction of high voltages in radar transmitter, protection against detection by radar detectors, significant improvement of range resolution, relevant reduction in clutter troubles and protection against jamming coming from spread spectrum action [1.3].

In pulse compression technique, the transmitted signal is frequency or phase modulated and the received signal is processed using a specific filter called "matched filter". In this form of pulse compression, a long pulse of duration T is divided into N sub pulses each of width τ. The phase of each sub-pulse is chosen to be either 0 or π radians. A matched filter is a linear network that maximizes the output peak-signal to noise ratio of a radar receiver which in turn maximizes the detectability of a target. In 1950-60, the practical realization of radars using pulse compression has taken place. At the starting, the realization of matched filters was difficult using traverse filters because of lack of delay line with enough bandwidth. Later matched filters have been realized by using dispersive networks

made with lumped-constant filters. In recent years, instead of matched filters, many sophisticated filters are in use.

The binary choice of 0 or π phase for each sub-pulse may be made at random. However, some random selections may be better suited than others for radar application. One criterion for the selection of a good "random" phase-coded waveform is that its autocorrelation function should have equal time side-lobes.Barker codes have called perfect codes because the highest side lobe is only one code element amplitude high.However,the largest pulse compression ratio that can be obtained with barker code is only 13 [1.4].

The codes that use any harmonically related phases on certain fundamental phase increments are called polyphase codes. Frank proposed a polyphase code called as Frank code which is more Doppler tolerant and has lower sidelobes than binary codes [1.8]. Krestschmer and Lewis have presented the variants of Frank code. P1 code which is derived from step frequency, Bolter matrix derived P2 code and linear frequency derived P3 and P4 codes. The significant advantage of P1 and P2 codes over the Frank code and the P4 code over P3 is that they are tolerant to receiver band limitations. [1.5, 1.6].

1.2. Motivation

The pulse compression in radar has major applications in the recent years. For better pulse compression, peak signal to sidelobe ratio should be as high as possible so that the unwanted clutter gets suppressed and should be very tolerant under Doppler shift conditions. Many pulse compression techniques have come into existence including neural networks. Most of the waveforms used for pulse compression generate random, noise-like sidelobe patterns, which make them hardly practical for sidelobe cancellation, the uniform sidelobe patterns of the Woo filter are promising for such a scheme.[1.7,1.8].Conventional sidelobe reduction techniques have suffered from performance degradation and SNR gains so asymmetrical weighting receivers can be use in such cases because they keep the sidelobe levels uniformly flat over all time delays while the range resolution loss is prevented [1.9]. The study of polyphase codes and their sidelobe reduction techniques are carried out since the polyphase codes have low sidelobes and are better Doppler tolerant and better tolerant to pre-compression bandlimiting.

1.3. Thesis Organization

Chapter-1 Introduction

Chapter-2 A Study of Polyphase Codes

This chapter deals with the introduction of Biphase codes and their limitations and different polyphase codes such as Frank, P1, P2, P3, P4 and complementary codes namely Golay complementary codes. The study of these codes, properties and their advantages over biphase codes is described

Chapter-3 Conventional Sidelobe Reduction techniques for polyphase codes

This chapter deals with the different Conventional sidelobe reduction techniques such as Amplitude weighting using different windows, TSSWA and an optimal technique for uniform range sidelobe and reduction of ISL. The study of these techniques and their properties are carried out.

Chapter-4 WOO Filter sidelobe reduction technique for pulse compression

This chapter describes the Woo filter concept of sidelobe reduction, the advanced versions of woo filter such as Woo form-I, Woo form-II, Asymmetrical weighting and a proposed pulse compression technique and described.

Chapter-5 Conclusion and scope for future work

The concluding remarks for all the chapters are presented in this chapter. It also contains some future research topics which need attention and further investigation**.**

Chapter 2

A Study of Polyphase Codes

2.1. Introduction

Radar is an electromagnetic system for detection and location of objects such as aircraft, ships, spacecraft, vehicles, people and natural environment [2.1]. It operates by radiating energy into space and detecting the echo signal reflected from object or target. The reflected energy that is returned to the radar not only indicates the presence of the target, but by comparing the received echo signal with the signal that was transmitted, its location can be determined along with other target-related information.

The basic principle of radar is simple. A transmitter generates an electro-magnetic signal (such as a short pulse of sine wave) that is radiated into space by an antenna. A portion of the transmitted signal is intercepted by a reflecting object (target) and is re-radiated in all directions. It is the energy re-radiated in back direction that is of prime interest to the radar. The receiving antenna collects the returned energy and delivers it to a receiver, where it is processed to detect the presence of the target and to extract its location and relative velocity. The distance to the target is determined by measuring the time taken for the radar signal to travel to the target and back. The range is

$$R = \frac{cT_R}{2} \tag{2.1}$$

Where T_R is the time taken by the pulse to travel to target and return, c is the speed of propagation of electromagnetic energy (speed of light). Radar provides the good range resolution as well as long detection of the target.

The most common radar signal or waveform is a series of short duration, somewhat rectangular-shaped pulses modulating a sine wave carrier [2.2]. Short pulses are better for range resolution, but contradict with energy, long range detection, carrier frequency and SNR. Long pulses are better for signal reception, but contradict with range resolution and minimum range. At the transmitter, the signal has relatively small amplitude for ease to generate and is large in time to ensure enough energy in the signal as shown in Figure 2.1. At the receiver, the signal has very high amplitude to be detected and is small in time [2.4].

A very long pulse is needed for some long-range radar to achieve sufficient energy to detect small targets at long range. But long pulse has poor resolution in the range dimension.

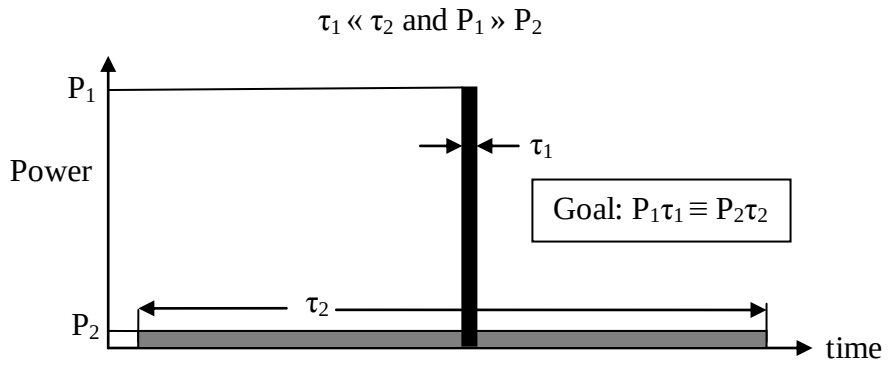

Figure 2.1 Transmitter and receiver ultimate signals

Frequency or phase modulation can be used to increase the spectral width of a long pulse to obtain the resolution of a short pulse. This is called "pulse compression".

2.2. Pulse Compression

The term radar signal processing incorporates the choice of transmitting waveforms for various radars, detection theory, performance evaluation, and the circuitry between the antenna and the displays or data processing computers. The relationship of signal processing to radar design is analogous to modulation theory in communication systems. Both fields continually emphasize communicating a maximum of information in a special bandwidth and minimizing the effects of interference.

Although the transmitted peak power was already in megawatts, the peak power continued to increase more and more due to the need of longer range detection. Besides the technical limitation associated with it, this power increase poses a financial burden. Not only that, target resolution and accuracy became unacceptable. Siebert [2.3] and others pointed out the detection range for given radar and target was dependent only on the ratio of the received signal energy to noise power spectral density and was independent of the waveform. The efforts at most radar laboratories then switched from attempts to construct higher power transmitters to attempts to use pulses that were of longer duration than the range resolution and accuracy requirements would allow.

Increasing the duration of the transmitted waveform results in increase of the average transmitted power and shortening the pulse width results in greater range resolution. Pulse

compression is a method that combines the best of both techniques by transmitting a long coded pulse and processing the received echo to get a shorter pulse.

The transmitted pulse is modulated by using frequency modulation or phase coding in order to get large time-bandwidth product. Phase modulation is the widely used technique in radar systems. In this technique, a form of phase modulation is superimposed to the long pulse increasing its bandwidth. This modulation allows discriminating between two pulses even if they are partially overlapped. Then upon receiving an echo, the received signal is compressed through a filter and the output signal will look like the one. It consists of a peak component and some side lobes.

2.3. Matched filter

A matched filter is a linear network that maximises the output peak-signal to noise (power) ratio of a radar receiver which in turn maximizes the detectability of a target. It is obtained by correlating a known signal, or a template, with an unknown signal to detect the presence of the template in the unknown signal. This is equivalent to convolving the unknown signal with a conjugated time-reversed version of the template. It is the optimal linear filter for maximizing the signal to noise ratio (SNR) in the presence of additive stochastic noise. It has a frequency response function which is proportional to the complex conjugate of the signal spectrum.

$$H(f) = G_a S^*(f) \exp(-j2\pi f t_m) \tag{2.2}$$

Where G_a is a constant, t_m is the time at which the output of the matched filter is a maximum (generally equal to the duration of the signal), and $S^*(f)$ is the complex conjugate of the spectrum of the (received) input signal s(t), found from the Fourier transform of the received signal s(t) such that

$$S(f) = \int_{-\infty}^{\infty} s(t) \exp(-j2\pi f t)\, dt \tag{2.3}$$

A matched filter for a transmitting a rectangular shaped pulse is usually characterized by a bandwidth B approximately the reciprocal of the pulse with τ or $B\tau \approx 1$. The output of a matched filter receiver is the cross-correlation between the received waveform and a replica of the transmitted waveform [2.5]

Instead of matched filter, an N-tap adaptive filter is used, by taking input as 13-bit barker code [1 1 1 1 1 -1 -1 1 1 -1 1 -1 1] and desired output as [12zeros 1 12zeros], and weights are trained using different adaptive filtering algorithms.

2.4. Phase coded pulse compression

In this form of pulse compression, a long pulse of duration T is divided into N sub-pulses each of width τ as shown in Figure 2.2. An increase in bandwidth is achieved by changing the phase of each sub-pulse. The phase of each sub-pulse is chosen to be either 0 or π radians or they can be harmonically related. The output of the matched filter will be a spike of width τ with an amplitude N times greater than that of long pulse. The pulse compression ratio is $N = T/\tau \approx BT$, where $B \approx 1/\tau$ = bandwidth. The output waveform extends a distance T to either side of the peak response, or central spike. The portions of the output waveform other than the spike are called time side-lobes. Phase coding can be either binary phase coding or polyphase coding.

2.4.1. Binary phase codes

The binary choice of 0 or π phase for each sub-pulse may be made at random. However, some random selections may be better suited than others for radar application. One criterion for the selection of a good "random" phase-coded waveform is that its autocorrelation function should have equal time side-lobes [2.1]. The binary phase-coded sequence of 0, π values that result in equal side-lobes after passes through the matched filter is called a Barker code. An example is shown in Figure 2(a). This is a Barker code of length 13. The (+) indicates 0 phase and (−) indicates π radians phase. The auto-correlation function, or output of the matched filter, is shown in Figure 2(b). There are six equal time side-lobes to either side of the peak, each of label 22.3 dB below the peak. The longest Barker code length is 13. The barker codes are listed in Table 2.1. When a larger pulse-compression ratio is desired, some form of pseudo random code is usually used. To achieve high range resolution with-out an incredibly high peak power, one needs pulse compression.

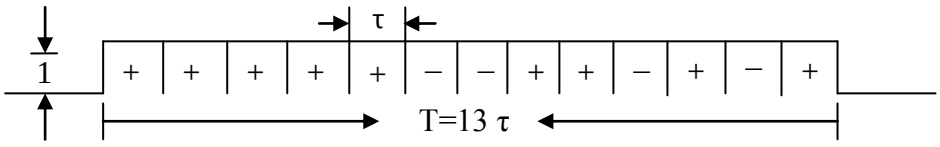

(a)

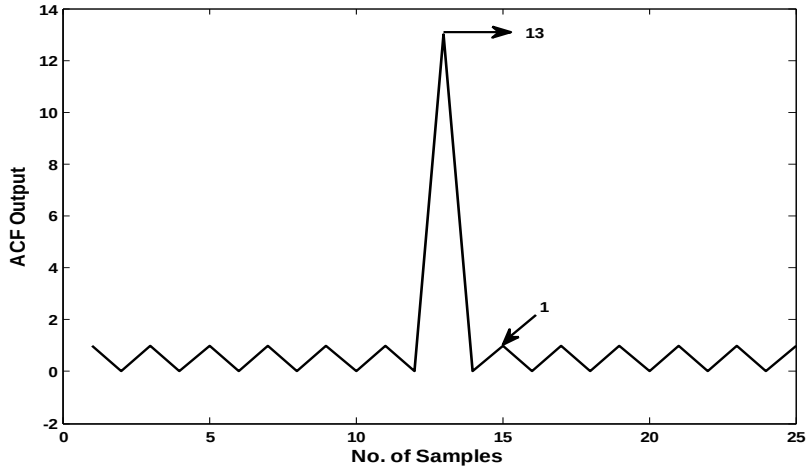

(b) Autocorrelation Output

Figure 2.2 (a) 13-element Barker Code

Table 2.1 Barker codes

Code Length	Code Elements	Sidelobe level, dB
2	+ −, + +	−6.0
3	+ + −	−9.5
4	+ + − +, + + + −	−12.0
5	+ + + − +	−14.0
7	+ + + − − + −	−16.9
11	+ + + − − − + − − + −	−20.8
13	+ + + + + − − + + − + − +	−22.3

Barker codes have been called the perfect codes because the highest sidelobe is only one code element amplitude high. However, the largest pulse compression ratio that can be obtained with the barker codes is only 13. The sidelobe levels obtained with the polyphase codes are not limited to any finite pulse compression ratio and exhibit better Doppler tolerance for broad range-Doppler coverage than do the biphase codes, and they exhibit relatively good side lobe characteristics [2.4].

2.5. Golay Complementary codes

Golay complementary codes [2.6] have properties that are useful in radar and communications systems. The sum of autocorrelations of each of a Golay complementary code pair is a delta function. This property can be used for the complete removal of sidelobes from radar signals, by transmitting each code, match–filtering the returns and combining them.

Consider two discrete binary sequences of length N, p1 (n) and p2(n), are termed Golay complementary sequences if the sum of their autocorrelations is zero except at zero lag, *i.e.*

$$R_{p_1}(k) + R_{p_2}(k) = 2N\delta(k) \tag{2.4}$$

Where the R_{p1}, R_{p2} are the autocorrelation of p_1 and p_2 codes respectively. The properties of golay complementary codes are as follows,

$$p_1(n),\ p_2(n)\ \in \{1, -1\},\ n = 1, 2, \ldots\ N \tag{2.5}$$

$$R_{p_1}(k) + R_{p_2}(k) = 2N, k = 0 \tag{2.6}$$

$$R_{p_1}(k) = -R_{p_2}(k),\ k \neq 0 \tag{2.7}$$

$$R_{p_1}(k)^2 = R_{p_1}(k)^2 \tag{2.8}$$

It is also the case that,

$$R_{p_1}(2k) = R_{p_2}(2k), \forall\ k \neq 0 \tag{2.9}$$

provided that the Golay sequences are constructed in a standard manner from a length–2 seed and are not permuted. A length–8 Golay pair and its complementary property is illustrated in Figure 2.3.

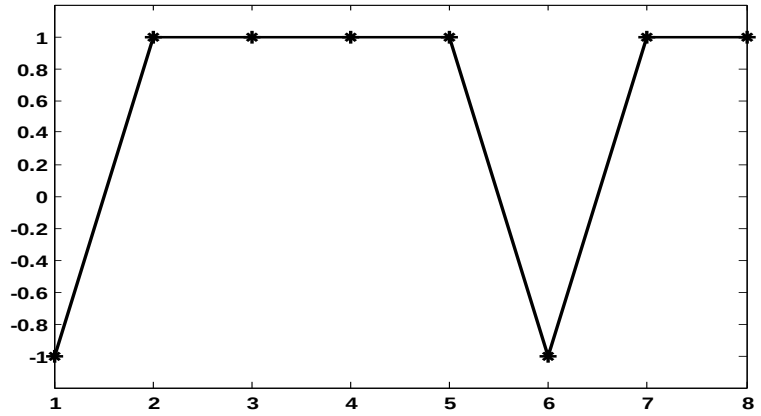
1
0.8
0.6
0.4
0.2
0
-0.2
-0.4
-0.6
-0.8
-1
1
2
3
4
5
6
7
8

(a)

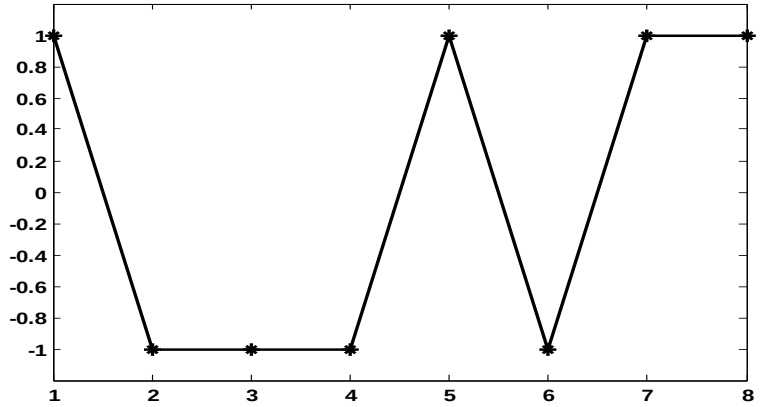
1
0.8
0.6
0.4
0.2
0
-0.2
-0.4
-0.6
-0.8
-1
1
2
3
4
5
6
7
8

(b)

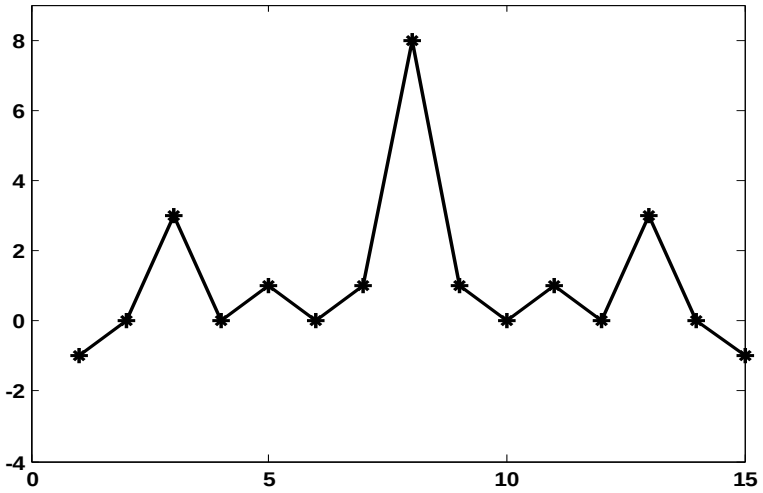
8
6
4
2
0
-2
-4
0
5
10
15

(c)

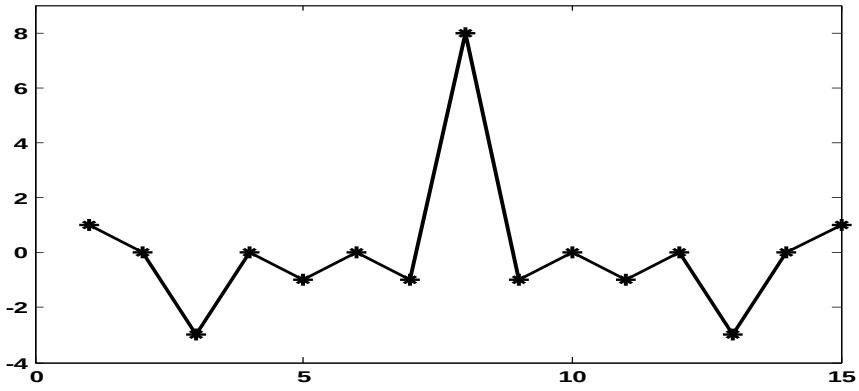

(d)

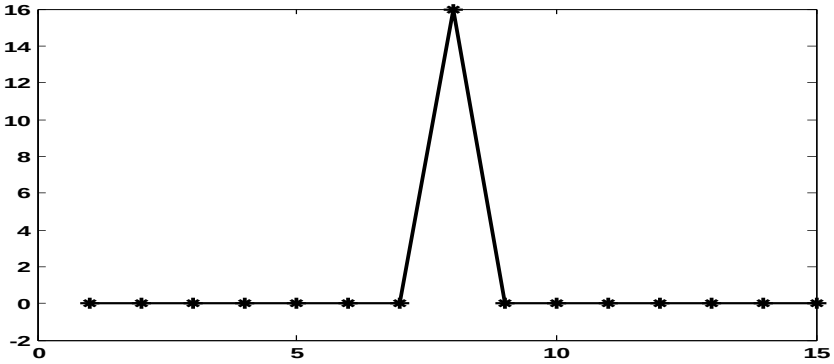

(e)

Figure 2.3. (a, b) Golay complementary codes (c,d) their respective autocorrelation functions (e) sum of the autocorrelations

2.5.1. Modified Golay Complementary Code

Let $p_1(n)$ and $p_2(n)$ be a Golay complementary pair. The modification is done for p2 code and the modified code q in terms of p_2 is expressed as

$$q(n) = p_2(n).e^{i\frac{\pi}{2}n} \tag{2.10}$$

The autocorrelations of original code p_2 and modified code q are related as follows

$$R_q(k) = R_{p_2}(k)e^{i\frac{\pi}{2}k} \tag{2.11}$$

The square of autocorrelation functions of p_1, p_2, and q are related as follows

$$R_q(k)^2 = R_{p_2}(k)^2 . e^{i\pi k}$$

$$= \begin{cases} -R_{p_1}(k)^2 , & if\ k\ is\ odd \\ 0 , & if\ k\ is\ even , k \neq 0 \\ R_{p_1}(k)^2 , & if\ k = 0 \end{cases} \quad (2.12)$$

And hence

$$R_q(k)^2 + R_{p_1}(k)^2 = 2N^2\delta(k) \quad (2.13)$$

From the above equation it is evident that the squares of autocorrelation functions of p_2 and q are complementary to each other. The complementarily of the modified golay code with the other code and its sum of squared autocorrelation functions are illustrated in Figure2.4.

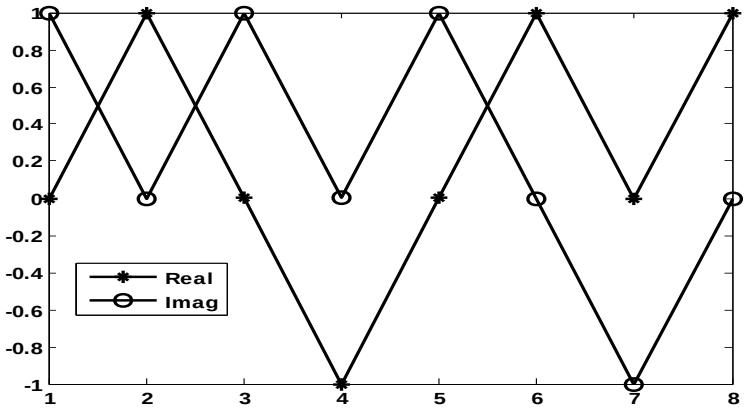

(a)

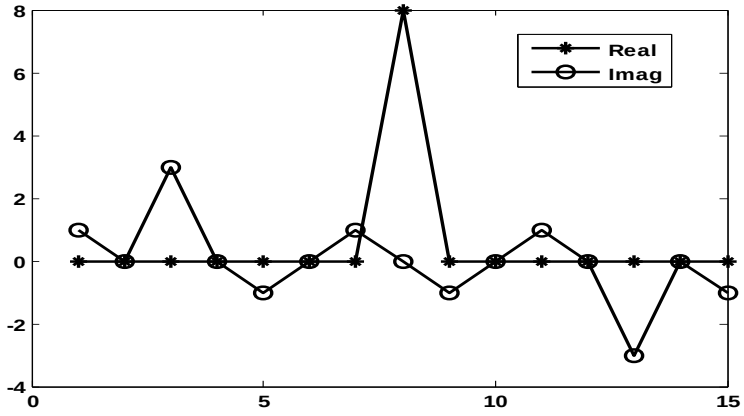

(b)

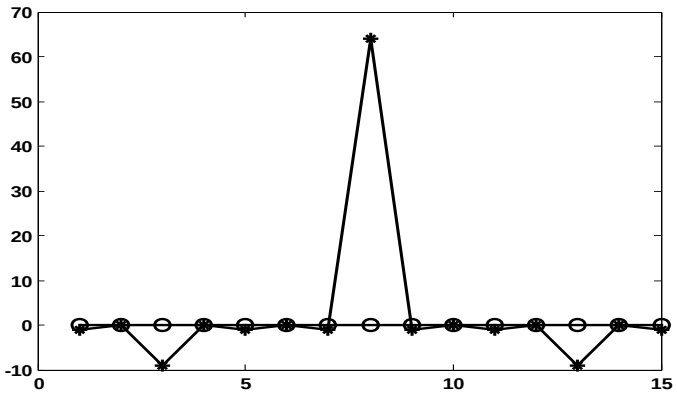

(c)

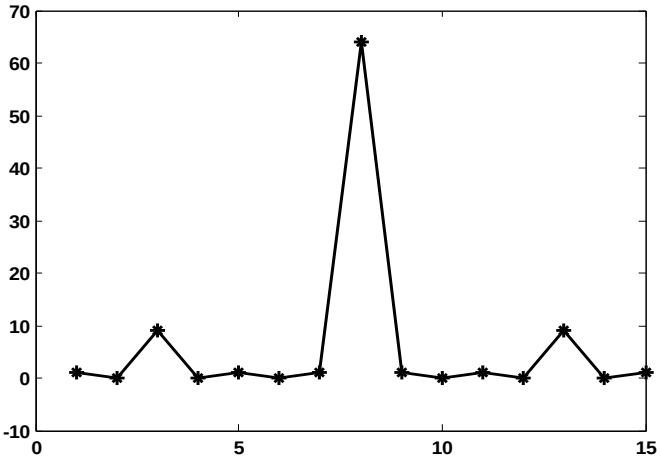

(d)

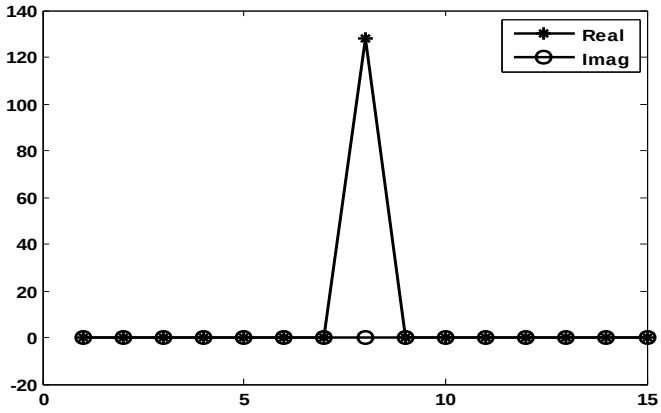

(e)

Figure 2.4. (a) Modified Golay code q (b) its autocorrelation function (c) its squared autocorrelation (d) squared autocorrelation of p_2 (e) sum of squared autocorrelations of q,p_2

Hence if both the sequences are multiplied by $e^{i\frac{\pi}{2}n}$ then they are complementary to each other but only one of the codes is multiplied by $e^{i\frac{\pi}{2}n}$ results in a pair which is complementary in the square [2.7].

Even though the Golay complementary codes provide complete sidelobe cancellation, they are not tolerant of Doppler shifts caused by targets moving relative to the radar. Hence we go for polyphase codes that have many applications which include low sidelobe levels, good Doppler tolerance for search radar applications and ease of implementation.

2.6. Polyphase codes

The codes that use any harmonically related phases based on a certain fundamental phase increment are called Polyphase codes and these codes are derived conceptually coherently detecting a frequency modulation pulse compression waveform with either a local oscillator at the band edge of the waveform (single side band detection) or at band center (double sideband detection) and by sampling the resultant inphase I and Q data at the Nyquist rate. The Nyquist rate in this case is once per cycle per second of the bandwidth of the waveform [2.8].

Frank proposed a polyphase code with good non-periodic correlation properties and named the code as Frank code [2.9]. Kretscher and Lewis proposed different variants of Frank polyphase codes called p-codes which are more tolerant than Frank codes to receiver bandlimiting prior to pulse compression [2.10, 2.11]. Lewis has proven that the sidelobes of polyphase codes can be substantially reduced after reception by following the autocorrelation with two sample sliding window subtractor for Frank and P1 codes and TSSWA for P3 and P4 codes.

Polyphase compression codes have been derived from step approximation to linear frequency modulation waveforms (Frank, P1, P2) and linear frequency modulation waveforms (P3, P4). These codes are derived by dividing the waveform into subcodes of equal duration, and using phase value for each subcode that best matches the overall phase trajectory of the underlying waveform. In this section the polyphase codes namely Frank, P1, P2, P3, P4 codes and their properties are described.

2.6.1. Frank Code

The Frank code is derived from a step approximation to a linear frequency modulation waveform using N frequency steps and N samples per frequency [2.9]. Hence the length of Frank code is N^2. The Frank coded waveform consists of a constant amplitude signal whose carrier frequency is modulated by the phases of the Frank code.

The phases of the Frank code is obtained by multiplying the elements of the matrix A by phase (2π/N) and by transmitting the phases of row1 followed by row 2 and so on.

$$A=\begin{bmatrix} 0 & 0 & 0 & \dots & 0 \\ 0 & 1 & 2 & \dots & (N-1) \\ 0 & 2 & 4 & \dots & 2(N-1) \\ 0 & 3 & 6 & \dots & 3(N-1) \\ . & & & & \\ . & & & & \\ 0 & (N-1) & 2(N-1) & \dots & (N-1)^2 \end{bmatrix} \tag{2.14}$$

The phase of the *i*th code element in the *j*th row of code group is computed as

$$\Phi_{i,j}=\left(\frac{2\pi}{N}\right)(i-1)(j-1) \tag{2.15}$$

Where *i* and *j* ranges from 1 to N. For example, the Frank code with N = 4, by taking phase value modulo 2π is given by the sequence,

$$\phi_{4x4}=\begin{bmatrix} 0 & 0 & 0 & 0 \\ 0 & \frac{\pi}{2} & \pi & \frac{3\pi}{2} \\ 0 & \pi & 0 & \pi \\ 0 & \frac{3\pi}{2} & \pi & \frac{\pi}{2} \end{bmatrix}$$

The autocorrelation function under zero Doppler, Doppler of 0.05 and the phase values of Frank code with length 100 are given in Figure 2.5.

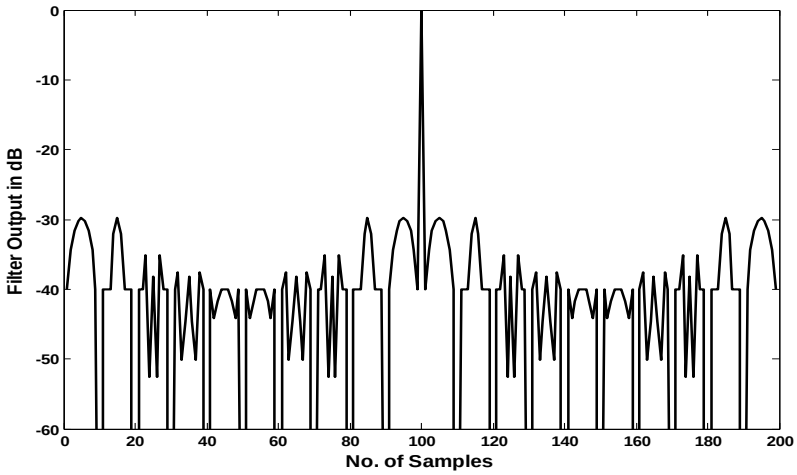

(a)

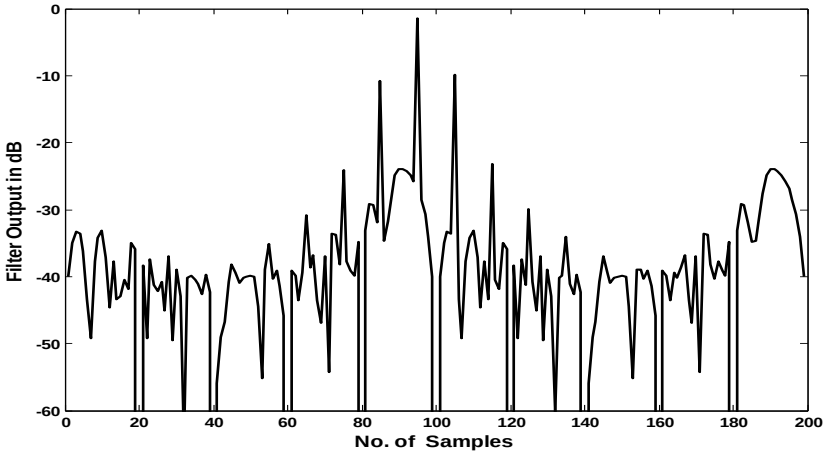

(b)

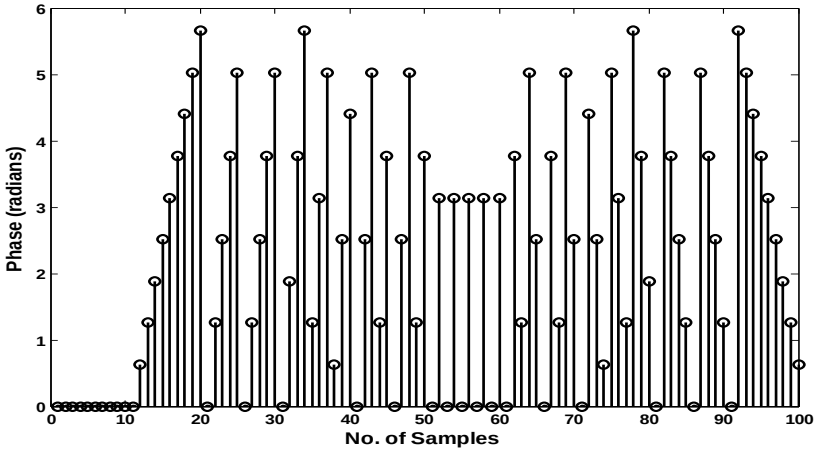

(Figure 2.5) Frank Code for length 100 (a) Autocorrelation under zero Doppler shift (b) Autocorrelation under Doppler = 0.05 (c) phase values

From the above figure it is evident that the Frank code has the largest phase increments from sample to sample in the center of the code. Hence, when the code is passed through a bandpass amplifier in a radar receiver, the code is attenuated more in the center of the waveform. This attenuation tends to increase the sidelobes of the Frank code ACF. Hence it is very intolerant to precompression bandlimiting. But comparing with binary phase codes, the Frank code has a peak sidelobe level (PSL) ratio of -29.79dB which is approximately 10 dB better than the best pseudorandom codes [2.10].

In the presence of Doppler shift, the autocorrelation function of Frank codes degrades at much slower rate than that for binary codes, however the peak shifts in position rapidly and a range error occurs due to this shift. The correlation under Doppler frequency f_d is obtained by correlating the transmitted one with received one multiplied by $e^{-j2\pi f_d T}$, where T is the length of the code. The PSL value under Doppler of 0.05 is calculated as -8.42dB.

2.6.2. P1 Code

The P1, P2, P3, P4 codes are obtained by the modified versions of the Frank code, with the dc frequency term in the middle of the pulse instead of at the beginning. P1 code is derived by placing the synchronous oscillators at the center frequency of the step chirp IF waveform and sampling the baseband waveform at the Nyquist rate [2.10].

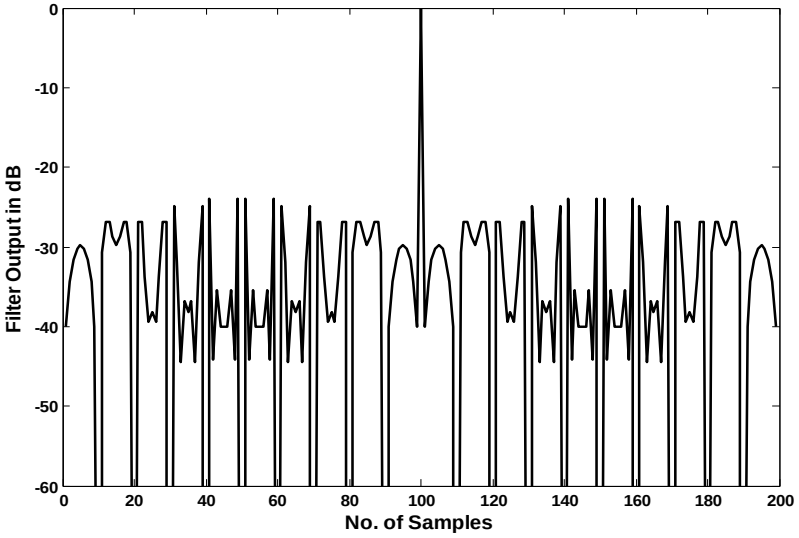

(a)

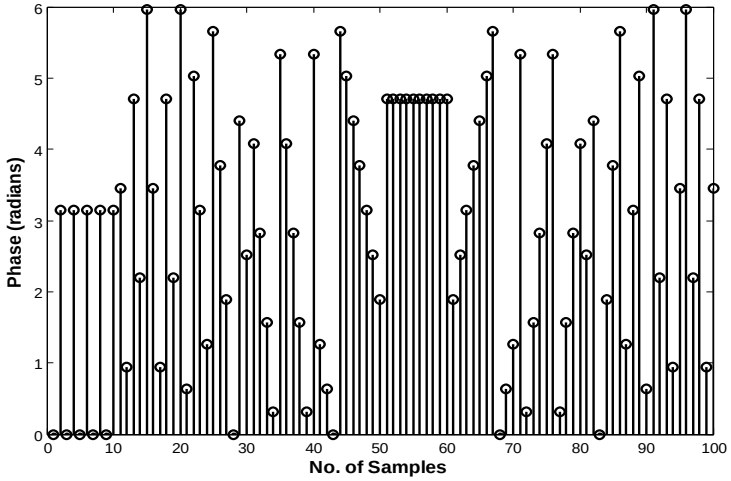

(b)

Figure 2.6. P1 Code for length 100 (a) its Autocorrelation (b) its phase values

The P1 code has N^2 elements and the phase of *i*th element of the *j*th group is represented as

$$\Phi_{i,j} = -\left(\frac{\pi}{N}\right)[N-(2j-1)][(j-1)N+(i-1)] \tag{2.16}$$

Where the integers *i* and *j* ranges from 1 to N. For example, the P1 code with N = 4, by taking phase value modulo 2π is given by the sequence,

$$\phi_{4x4} = \begin{bmatrix} 0 & \pi & 0 & \pi \\ \frac{5\pi}{4} & \frac{3\pi}{4} & \frac{\pi}{4} & \frac{7\pi}{4} \\ \frac{\pi}{2} & \frac{\pi}{2} & \frac{\pi}{2} & \frac{\pi}{2} \\ \frac{7\pi}{4} & \frac{\pi}{4} & \frac{3\pi}{4} & \frac{5\pi}{4} \end{bmatrix}$$

The autocorrelation function and the phase values of P1 code with length 100 are given in Figure 2.6. The PSL value is obtained as -23.99dB. P1 code has the highest phase increments from sample to sample at the two ends of the code. Thus, when waveforms phase coded with these codes are passed through band pass amplifiers in a radar receiver, P1 code is attenuated most heavily at the two ends of the waveform. This reduces the sidelobes of the P1 code autocorrelation function. Hence this exhibits relatively low sidelobes than Frank code. This result shows that P1 code is very precompression bandwidth tolerant than Frank code.

Also, P1 code has an autocorrelation function magnitude which is identical to the Frank code for zero Doppler shifts.

2.6.3. P2 Code

The P2 code has the same phase increments within each phase group as the P1 code, except that the starting phases are different [2.10]. The P2 code has N^2 elements and the phase of *i*th element of the *j*th group is represented as

$$\Phi_{i,j} = \left(\frac{\pi}{2N}\right)[N - 2i + 1][N - 2j + 1] \tag{2.17}$$

Where *i* and *j* are integers ranges from 1 to N.The value of N should be even in order to get low autocorrelation sidelobes. An odd value of N results in high autocorrelation sidelobes. For example, the P2 code with N = 4, by taking phase value modulo 2π is given by the sequence,

$$\phi_{4x4} = \begin{bmatrix} \frac{9\pi}{8} & \frac{3\pi}{8} & \frac{13\pi}{8} & \frac{7\pi}{8} \\ \frac{3\pi}{8} & \frac{\pi}{8} & \frac{15\pi}{8} & \frac{13\pi}{8} \\ \frac{13\pi}{8} & \frac{15\pi}{8} & \frac{\pi}{8} & \frac{3\pi}{8} \\ \frac{7\pi}{8} & \frac{13\pi}{8} & \frac{3\pi}{8} & \frac{9\pi}{8} \end{bmatrix}$$

The autocorrelation function under zero Doppler, Doppler of 0.05 and the phase values of P2 code with length 100 are given in Figure 2.7.

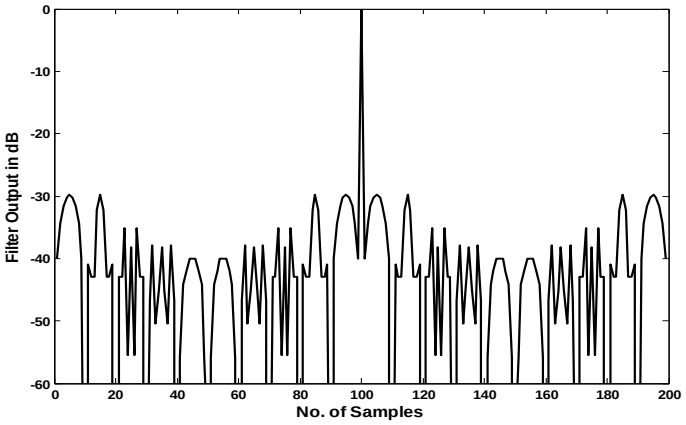

(a)

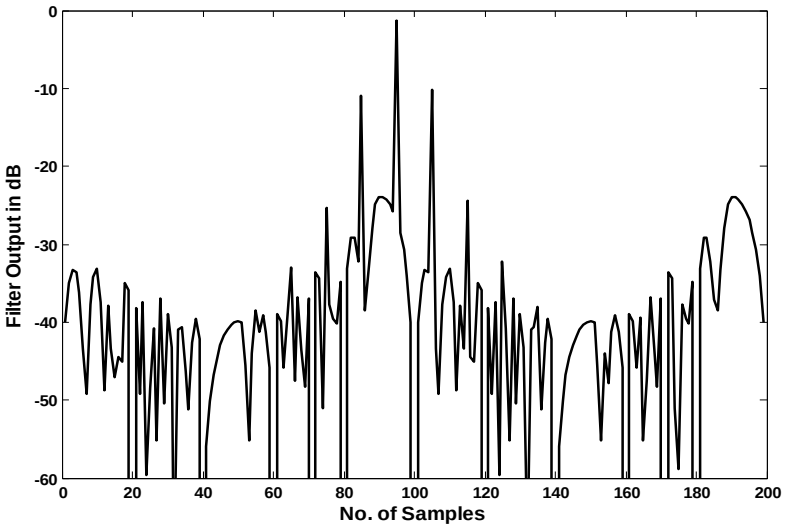

(b)

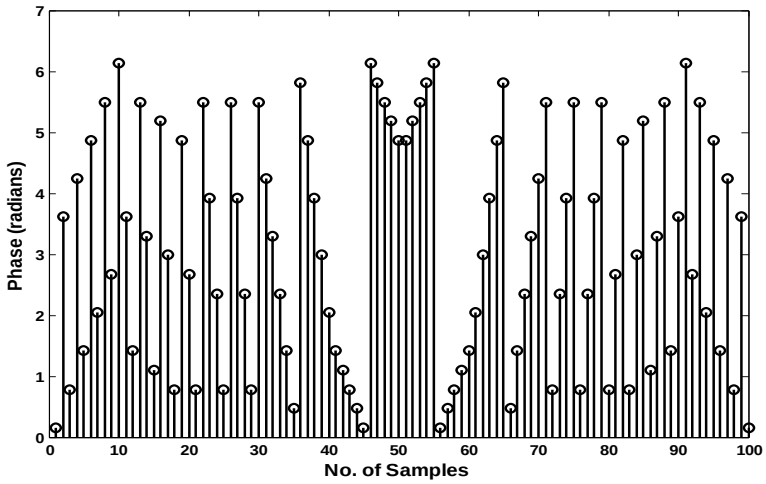

(c)

Figure 2.7. P2 Code for length 100 (a) Autocorrelation under zero doppler shift (b) Autocorrelation under doppler = 0.05 (c) phase values

The peak sidelobes of the P2 code are the same as the Frank code for zero Doppler case and the mean square sidelobes of the P2 code are slightly less. The value of PSL obtained as -29.79dB which is same as that of Frank code. Under Doppler of 0.05 the PSL value is computed as -8.79dB which is slightly lower than that of Frank code. The phase changes in P2 code are largest towards the end of the code.

The significant advantage of the P1 and P2 codes over the Frank code is that they are more tolerant of receiver band limiting prior to pulse compression. But P1 and P2 suffers from high PSL value. PSL value is obtained by the ratio of peak sidelobe amplitude to the main lobe amplitude. To obtain low PSL values, we go for P3 and P4 codes.

2.6.4. P3 Code

The P3 code is conceptually derived by converting a linear frequency modulation waveform to baseband using a local oscillator on one end of the frequency sweep and sampling the inphase I and quadrature Q video at the Nyquist rate [3.11]. Letting the waveform to be coherently detected have a pulse length T and frequency

$$f = f_0 + kt \tag{2.18}$$

Where k is a constant, the bandwidth of the signal will be approximately

$$B = kT \tag{2.19}$$

This bandwidth will support a compressed pulse length of approximately

$$t_c = 1/B \tag{2.20}$$

And the waveform will provide a pulse compression ratio of

$$\delta = T/t_c \tag{2.21}$$

Assuming that the first sample of I and Q is taken at the leading edge of waveform, the phases of successive samples taken t_c apart is

$$\Phi_i^{p3} = 2\pi \int_0^{(i-1)tc} [(f_0 + kT) - f_0]dt$$

$$= \pi(i-1)^2 t_c^2 \tag{2.22}$$

Thus the phase sequence of the P3 signal is given by

$$\Phi_i = \frac{\pi}{N}(i-1)^2 \tag{2.23}$$

Where i varies from 1 to N and N is the compression ratio. For example, the P3 code with N = 16, by taking phase value modulo 2π is given by the sequence,

$$\Phi_{16} = \left[0 \quad \frac{\pi}{16} \quad \frac{4\pi}{16} \quad \frac{9\pi}{16} \quad \pi \quad \frac{25\pi}{16} \quad \frac{4\pi}{16} \quad \frac{17\pi}{16} \quad 0 \quad \frac{17\pi}{16} \quad \frac{4\pi}{16} \quad \frac{25\pi}{16} \quad \pi \quad \frac{9\pi}{16} \quad \frac{4\pi}{16} \quad \frac{\pi}{16}\right]$$

The autocorrelation function and the phase values of P3 code with length 100 are given in Figure 2.8. The PSL value is obtained as -26.32dB.

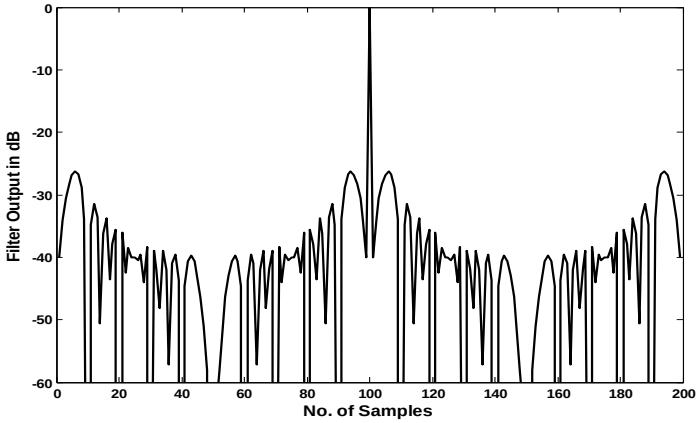

(a)

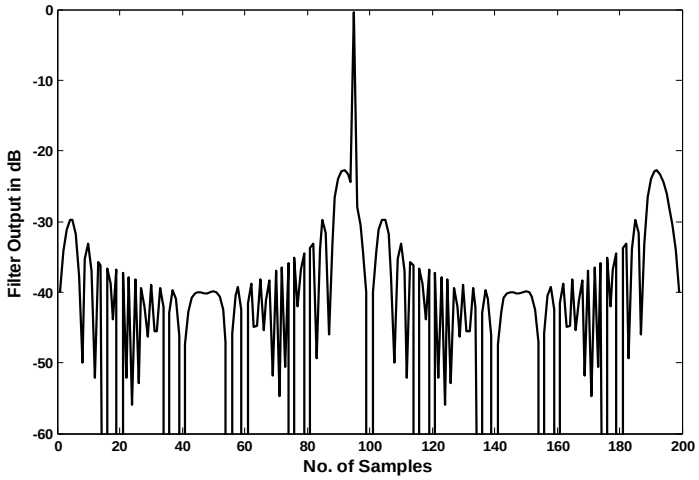

(b)

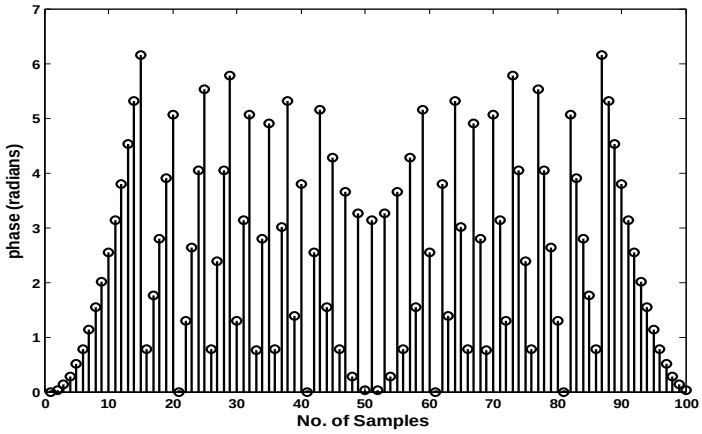

(c)

Figure 2.8. P3 Code for length 100 (a) Autocorrelation under zero Doppler shift (b) Autocorrelation under doppler = 0.05 (c) phase values

The peak side lobe ratio for P3 code is a bit larger than the Frank, P1, P2 codes. In the P3 code, the largest phase increments occur at the center of the code. Hence the P3 code is not precompression bandwidth limitation tolerant but is much more Doppler tolerant than the Frank or P1 and P2 codes.

2.6.5. P4 Code

The P4 Code is conceptually derived from the same waveform as the P3 Code[2.10,2.11]. However, in this case, the local oscillator frequency is set equal to $f_0 + kT/2$ in the I,Q detectors. With the frequency, the phases of successive samples taken t_c apart are

$$\Phi_i^{p4} = 2\pi \int_0^{(i-1)tc} [(f_0 + kt) - (f_0 + \frac{kT}{2})]dt$$

$$= 2\pi \int_0^{(i-1)tc} k\left(t - \tfrac{T}{2}\right) dt \qquad (2.24)$$

Or $$\Phi_i^{p4} = \pi k(i-1)^2 tc^2 - \pi kT(i-1)^2 tc^2$$

$$= [\pi(i-1)^2/\delta] - \pi(i-1) \qquad (2.25)$$

Thus the phase sequence of the P4 signal is given by

$$\Phi_i = \frac{\pi}{N}(i-1)(i-N-1) \qquad (2.26)$$

Where i varies from 1 to N and N is the compression ratio. For example, the P4 code with N = 16, by taking phase value modulo 2π is given by the sequence,

$$\Phi_{16} = \left[0 \quad \frac{17\pi}{16} \quad \frac{4\pi}{16} \quad \frac{25\pi}{16} \quad \pi \quad \frac{9\pi}{16} \quad \frac{4\pi}{16} \quad \frac{\pi}{16} \quad 0 \quad \frac{\pi}{16} \quad \frac{4\pi}{16} \quad \frac{9\pi}{16} \quad \pi \quad \frac{25\pi}{16} \quad \frac{4\pi}{16} \quad \frac{17\pi}{16}\right]$$

The autocorrelation function under zero Doppler, Doppler of 0.05 and the phase values of P4 code with length 100 are given in Figure 5.7. The PSL value is obtained as -26.32dB under zero Doppler, and -22.31dB under Doppler of 0.05 which are similar to P3 code.

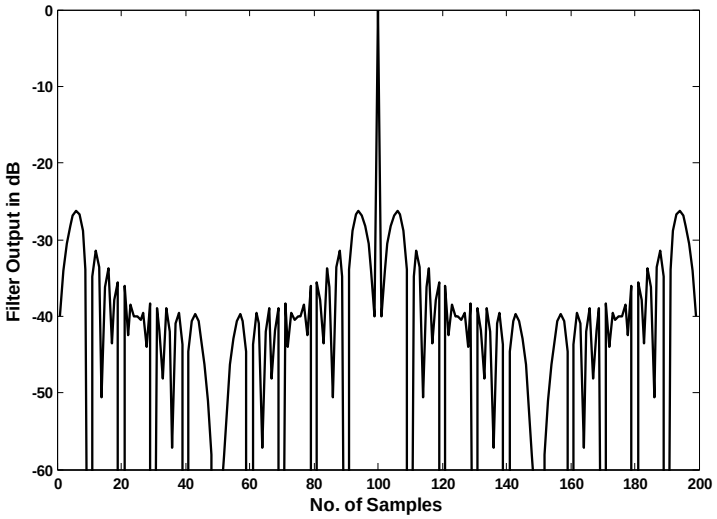

(a)

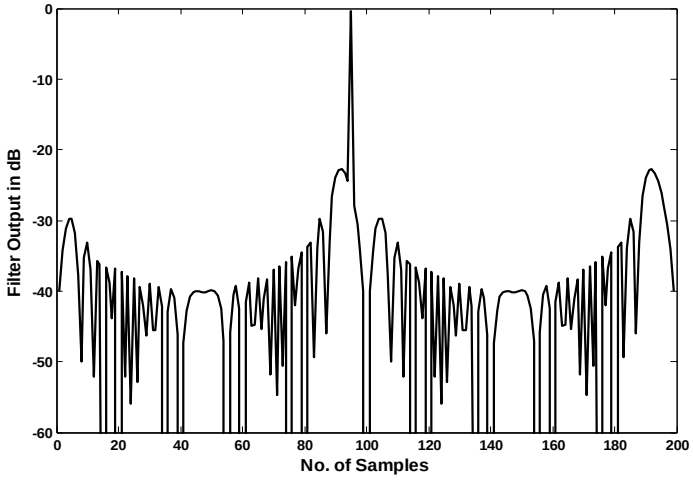

(b)

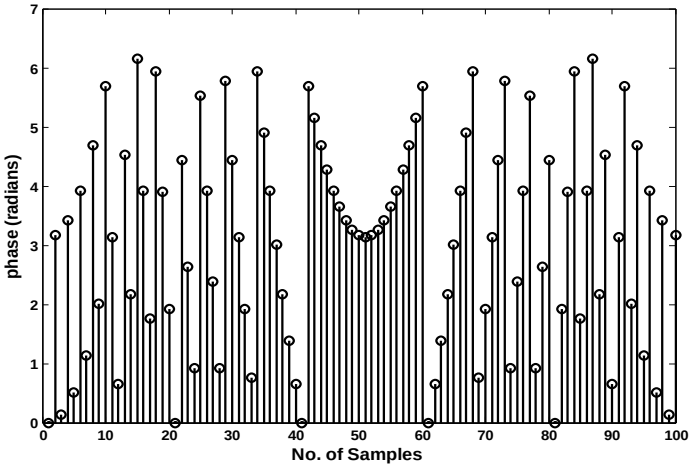

(c)

Figure 2.9. P4 Code for length 100 (a) Autocorrelation under zero Doppler shift (b) Autocorrelation under Doppler = 0.05 (c) phase values

The largest phase increments from code element to code element are on the two ends of the P4 code but are in the middle of the P3 code [2.12]. Thus the P4 code is more precompression bandwidth limitation tolerant but has same Doppler tolerance than the P3 code. This follows since precompression bandwidth limitations average the code phase increments and would attenuate the P4 code on the ends and the P3 code in the middle. The former increases the peak-to-sidelobe ratio of the compressed pulse while the latter decreases it.

2.7. Summary

In this chapter, Phase coded pulse compression, Binary phase codes, Golay complementary codes and polyphase codes are described. The performances of polyphase codes namely Frank, P1, P2, P3, P4 codes, their autocorrelation properties, their phase values and their properties under Doppler shift conditions are discussed.

Chapter 3

Conventional Sidelobe Reduction Techniques for Polyphase Codes

3.1 Range Time Sidelobes

Sidelobes are unwanted because a time sidelobe of a strong echo may hide a weaker target return. Also any clutter present in the sidelobes can leak into range of interest. Most of the energy will be wasted in the sidelobes .Hence detection becomes weaker.[3.1] Range-time sidelobes are the result of convolving the radar return with the non-ideal filter response (i.e. some energy remains outside the desired pulse bandwidth), This results in the "blurring" of returns in range near high reflectivity gradients, like ground clutter.

3.2 Sidelobe Structure

The sidelobe structure of the compressed waveform employing the referenced polyphase codes can best be understood by understanding the logic employed in the compression process. This logic is show in Figures 3.1 in a simplified but rigorously correct embodiment.

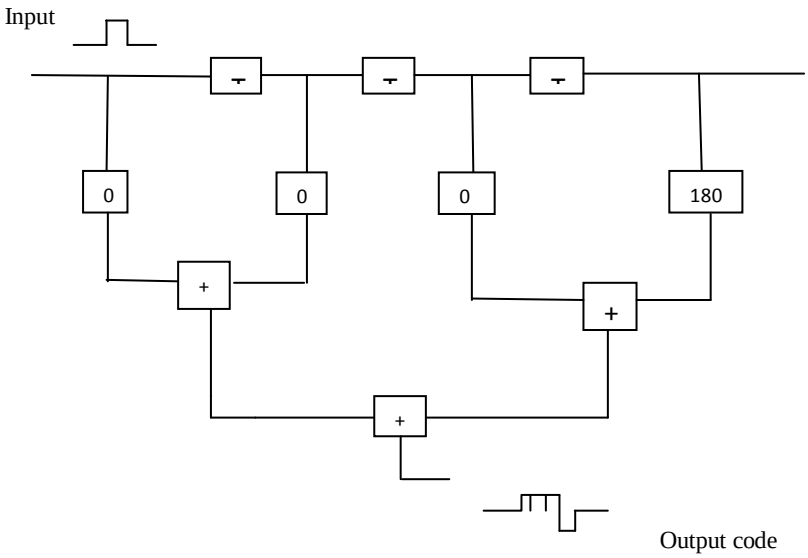

(a)

Figure 3.1(a). N=2 Frank code generator

This figure shows a circuit for digitally generating a Frank code with N=2 and pulse compression ratio (N)(N)=4.In this circuit, T signifies a delay a length T, the number in the boxes fed by taps on the delay line are the phase shifts in degrees that are introduced by the coxes and the boxes

with plus signs in them are adders. In this circuit, the signals are assumed to be inphase I and quadrature Q pulses of length T on parallel lines that are not shown for simplicity.

The input pulse can be a unit amplitude in *I* and zero in *Q* representing a complex number. The put frequency phase for j=1 and j=2(1), are then 0,0adn 0,180 show in video form as output code.

Figure 3.1(b) illustrates pulse compression. It shows the pulse compression code time –reversed entering the normal output of the code generator after being conjugated. The conjugation of a 0 phase signal produces a 0 phase signal and that the conjugation of a 180 deg signal produces a 180 deg signal. This is because conjugation is done by changing the sign of the Q term in the complex number representing the phase, i.e., changing +Q to –Q.

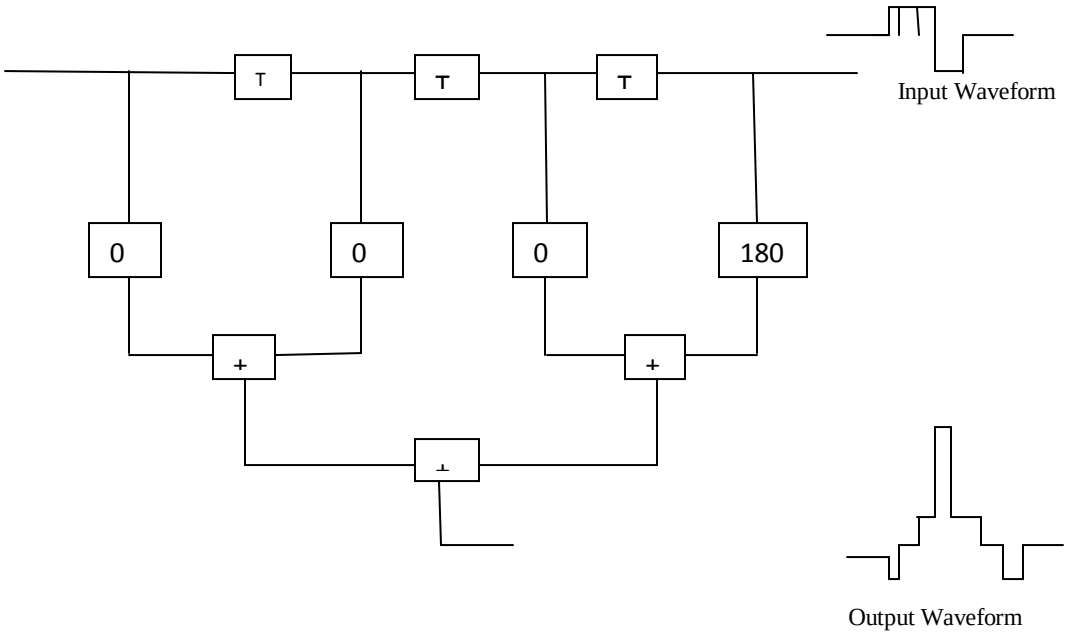

(b)

Figure 3.1(b) N=2 Frank code modulated waveform compressor

This figure also shows compressed pulse output obtained from the pulse compressor starting with unit magnitude negative pulse followed by a zero magnitude pulse, then a unit magnitude positive pulse and finally, by the compressed pulse peak having a magnitude of positive 4.It

should be noted that the compressed pulse peak also has trailing sidelobes that are the mirror image of the leading sidelobes.

With relatively large pulse compression ratios r, the farthest out and closest in sidelobes are equal to or larger than any sidelobe in the compressed pulse-compression-waveform. This is illustrated in Fig 3.2.

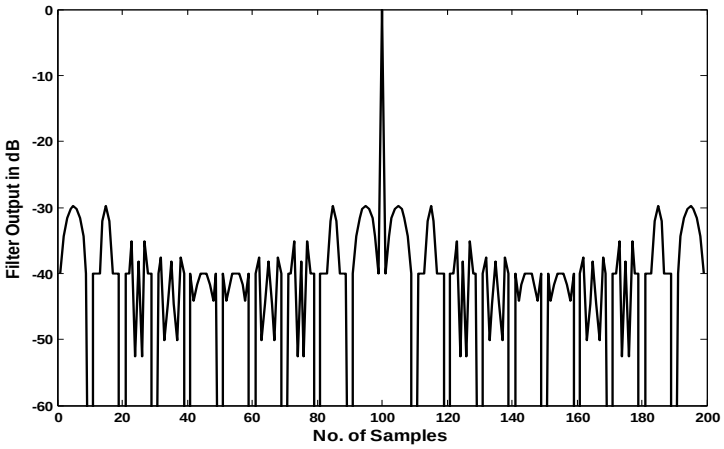

Figure 3.2 Compressed pulse of Frank code with r = 100

Which shows the compressed pulse waveform power of an r = 100 Frank code. The highest sidelobes are 30dB = π (π) r down from the pulse compression peak. This is characteristic of both the Frank and P1 codes. This peak (p) to highest sidelobe (HSL) power ratio of these codes is approximately

$$P/HSL = \pi\,(\pi)\, r \tag{3.1}$$

The derivation of this value proceeds as follows. The phase increments of the lowest frequency Frank code group (j=1) are 0 degrees and the phase increments of the highest frequency code group with j=N are (N-1)360/N = -360/N deg

Thus, as the conjugate lowest-frequency code group indexes into the highest frequency code group generator as shown in (Fig 3.1(b)). The first pulse will have a phase of 0 deg. It will be phase shifted by - (360/N) (N-1) =+ (360/N) deg and will exit the compressor as the first proceeding –sidelobe of unit amplitude. The second pulse in will also have 0 deg phase; it will be phase shifted by + (360/N) deg and will be added to the first pulse in phase shifted by 2(360/N)

deg. This will produce a sidelobe that is the vector sum of unit vector of phase 360/N deg and 2(360/N) deg. This multiple vector summing will continue until the complete lower frequency of the Frank code indexes in to the compressor.

At this time, the vector inputted, phase shifted and added form and approximate to a circle with a perimeter of N unit magnitude as show in Figure 3.3

The diameter of this circle will be N/π and will be the peak of the farthest out sidelobe. Since the peak of the pulse compressed waveform will be (N) (N) and the highest sidelobe peak will be (N/π), the peak squared to highest sidelobe peak squared ratio will be

$$(P/HSL)(P/HSL)= [N (N)] [N (N)]/ [(N (N)]/\pi (\pi) = \pi (\pi) r \qquad (3.2)$$

Equation (3.2) justifies (3.1) for Frank code .Also however, that the P1 code j=1and j=N code groups differ from those of Frank code.

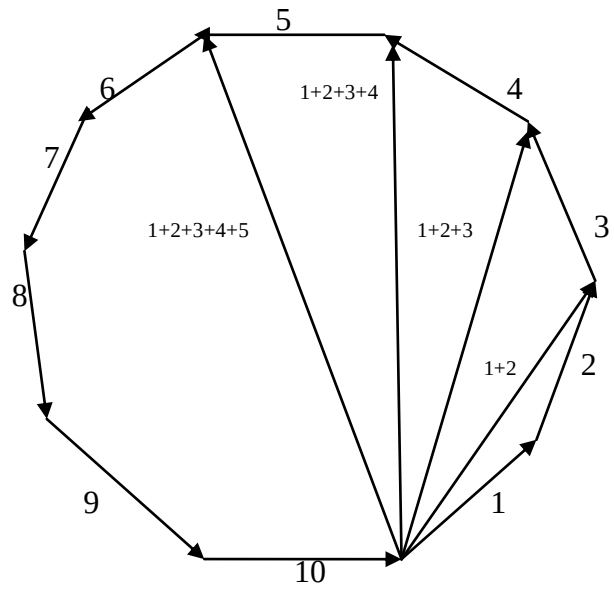

Figure 3.3 Derivation of peak value of farthest out sidelobe of an r=100 Frank coded waveform

Instead of the phase increments within the lowest and highest frequency groups of the P1 code being small as in Frank code, they differ by only small values from 180 deg in large compression-ratio codes. This causes successive samples of the P1 autocorrelation function to differ in phase by nearly 180 deg instead of being nearly in phase as in the Frank code example

shown in fig 3.2.They have the same magnitude however as those of the Frank code .Thus (3.2) also gives the right value for the P1 code.

The farthest out and closest in sidelobe of the P3 and P4 code (Fig 3.4) are also the largest sidelobe in compressed waveform. However, the peak squared to highest sidelobe squared ratio in not given by (3.2). This is because the P3 and P4 codes are derived from a linear-frequency-modulation waveform instead of a step-approximation to a linear-frequency waveform like the Frank and P1 code [3.2].

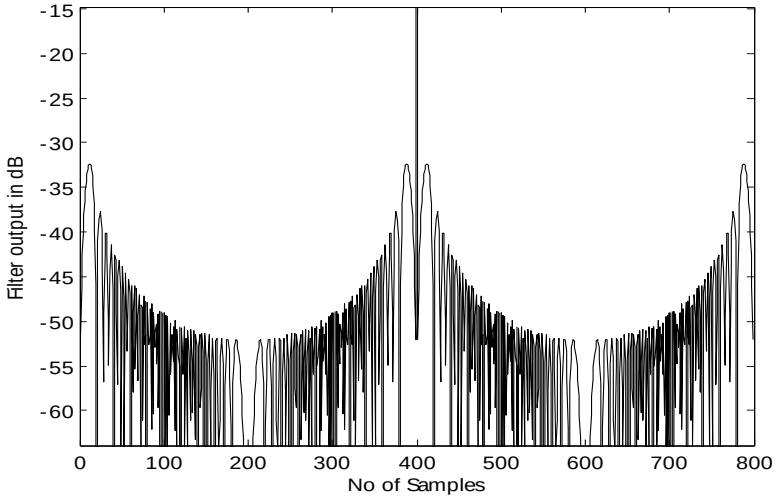

Figure 3.4 P3 code 400 to 1 compressed pulse.

The highest sidelobes of the P3 and P4 codes are on the order of

$$\left(\frac{P}{HSL}\right)\left(\frac{P}{HSL}\right)_{p3,p4} = 4r \tag{3.3}$$

Or 32 dB in Fig 3.4 where r=400.

3.3 Performance measures

The performance measures of Pulse Compression techniques are Peak side level (PSL), integrated sidelobe (ISL), SNR loss and Doppler shift [3.5].

3.3.1. Peak Sidelobe Ratio

It is the ratio of the maximum of the sidelobe amplitude to mainlobe amplitude

$$PSL = 20log_{10}[\max\left\{\frac{r(i)}{r(0)}\right\}]_{i\neq 0} \tag{3.4}$$

3.3.2. Integrated sidelobe ratio

It the ratio of the energy of Autocorrelation function of sidelobes to the total energy of the Autocorrelation function of the mainlobe [3.3].

$$ISL = 10log_{10} \sum_{i=-L}^{L}\{r(i)/r(0)\}^2 \tag{3.5}$$

3.3.3. SNR Degradation

SNR degradation per dB is the ratio of mainlobe peak amplitude without Doppler shift to mainlobe peak amplitude with Doppler shift.

$$SNR = \left[\frac{\sum_{n=1}^{N} a_{n+k}^{*} a_n}{\sum_{n=1}^{N} a_n \ e^{j2\pi nfdtc} a_{n+k}^{*}}\right] \tag{3.6}$$

3.4 Sidelobe Reduction Techniques

3.4.1 Two Sample Sliding Window Adder (TSSWA)

TSSWA is applied for polyphase codes in order to reduce the PSL values. It is a new type of pulse compression technique that compresses the pulse to the width of several subpulse and not to the width of single subpulse by reducing bandwidth [3.2].

The TSSWA is added after the autocorrelation of the code. The block diagram of autocorrelation followed by single TSSWA and double TSSWA are shown in Figure 3.5. The spectrum bandwidth of the coded signal is approximately the inverse of the subpulse width τ in the conventional autocorrelation output which is given in Figure 3.6(a). Hence the pulse is then compressed to a single subpulse. The function of TSSWA is to divide the signal into two, delay one of them by τ and add it to the other one. The output of the autocorrelation followed by a single TSSWA is given in Figure 3.6(b).

The compressed width after single TSSWA will be 2τ. Further if again one more TSSWA is added to single TSSWA output then autocorrelation followed by double TSSWA is formed and its output has compressed width of 3τ as shown in Figure 3.6(c). From the spectral point of view, the TSSWA is carried out once, if the weighting function $(1+\cos\omega\tau)$ is multiplied by the spectral intensity of the input signal so that bandwidth becomes narrowed. For double TSSWA, the weighting function $(1+\cos\omega\tau)^2$ is multiplied by the spectral intensity of the input signal so that the signal bandwidth becomes narrower and so on.

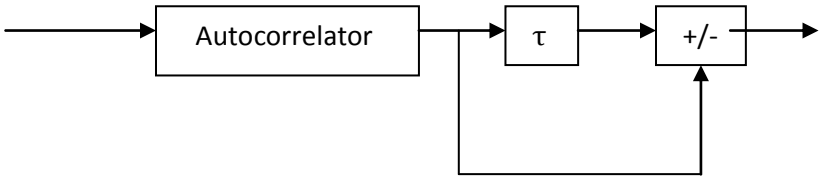

(a)

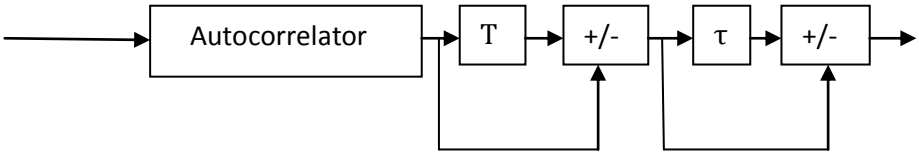

(b)

Figure 3.5 (a) Auto-Correlator followed by single TSSWA (b) Auto-Correlator followed by double TSSWA

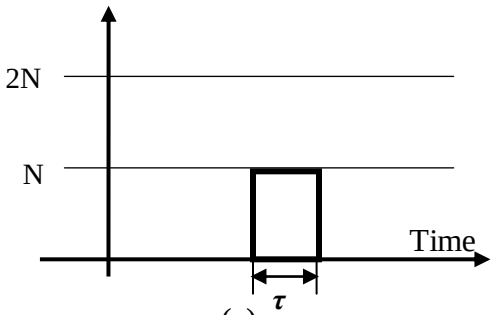

(a)

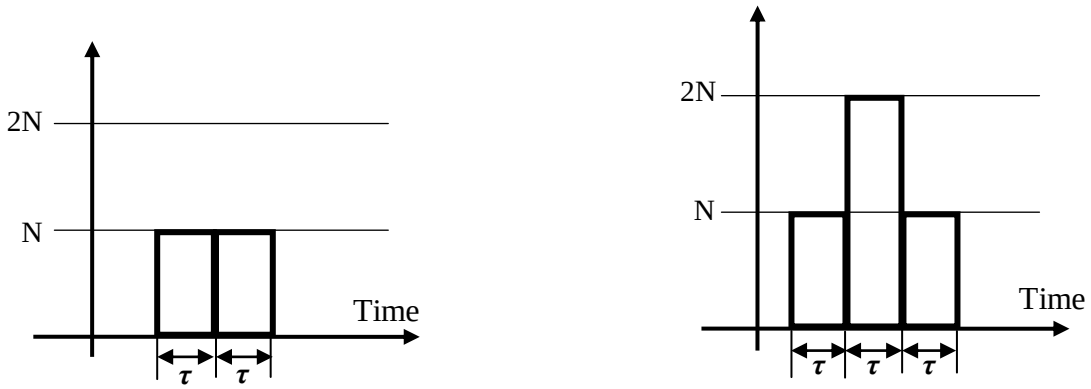

(b) (c)

Figure 3.6 (a) Correlator output (b) Single TSSWA output (c) Double TSSWA output

The vector addition of the phase shifted outputs of the delays and the phase shifted input to the delay line in the pulse compression process can only change sidelobe amplitude by about the magnitude of the last pulse in (Fig 3.3).This the basis of the technique for reducing the range-time-sidelobes magnitude of the polyphase pulse compression codes discussed here.

Different techniques however must be used for the codes that result from single sideband derived codes like the Frank or P3 codes, the successive samples of large sidelobes have nearly the same phase and differ from each other on the order of one code element. Thus, it is possible to limit the sidelobes of the compressed waveform to one code element magnitude by employing a sliding window two-sample subtractor in the output of the pulse compressor as illustrated in Fig 3.5. This sliding window subtractor is a one-sample delay T whose input and output drive the two inputs of a subtractor or adder.

Fig 3.7 shows the effect of two-sample sliding window subtractor on the compressed pulse shown in Fig 3.4 The highest sidelobe in Fig 3.7 is 46dB and that the effective pulse compression ratio is only 200 to 1 due to the subtractor. The power ratio between a code element and the mainlobe peak with a pulse compression ratio of 200to 1 is 46dB.The 46dB sidelobe peaks in Fig 3.7 are thus only one effective code element magnitude and are equivalent to the barker code element magnitude and are equivalent to the barker code level.

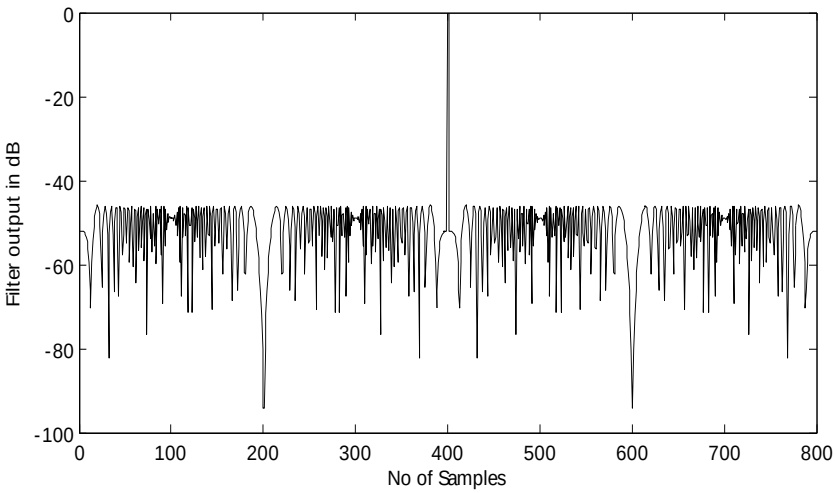

Figure 3.7 P3 code compressed pulse with two-sample sliding window subtractor

This finding justifies the statement that the sliding window two-sample subtractor limits the highest pulse compression sidelobe power to that of one code element.

Figure 3.8 shows the effect of two-sample sliding window adder in place of the two-sample sliding window subtractor used in Fig 3.7.The adder doubled the sidelobe magnitude and quadrupled the power without affecting the mainlobe peak power. It also doubled the peak width and halved the pulse compression ratio.

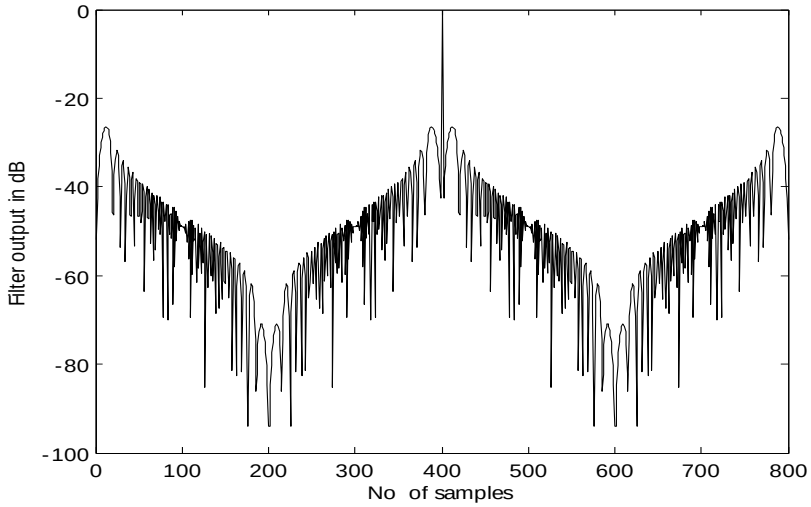

Figure 3.8 Result of two-sampling window adder on output of 400 to 1 P3 code

In the case of the double sideband derived codes successive samples of the highest sidelobes in the compressed waveform out of the compressor are nearly 180 deg out of phase and differ in magnitude by about one code element magnitude.

As ad consequence, their sidelobes may be limited to amplitude s of only one code element by using a two-sample sliding window adder on the output of the compressor. Fig 3.9 illustrates a compressed P4 code with a pulse compression ratio of 400 to 1.

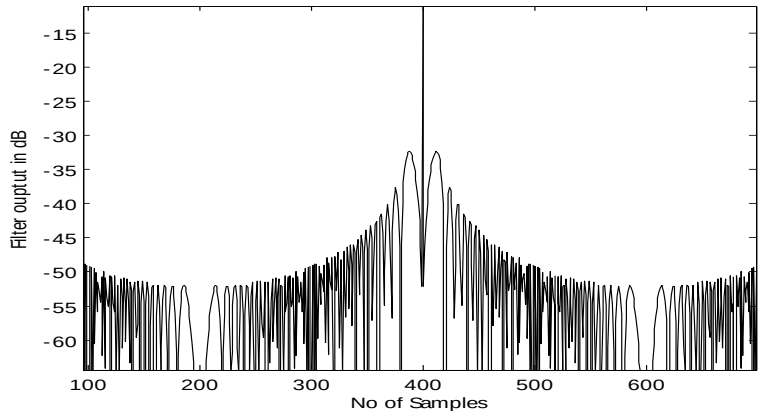

Figure 3.9 Compressed P4 code with 400 to 1 pulse compression ratio

Figure 3.10 shows the result of a two-sample sliding window adder. The adder reduces all sidelobes peaks to 46dB, i.e. to one code element magnitude or less with and effective pulse compression ratio of 200 to1.

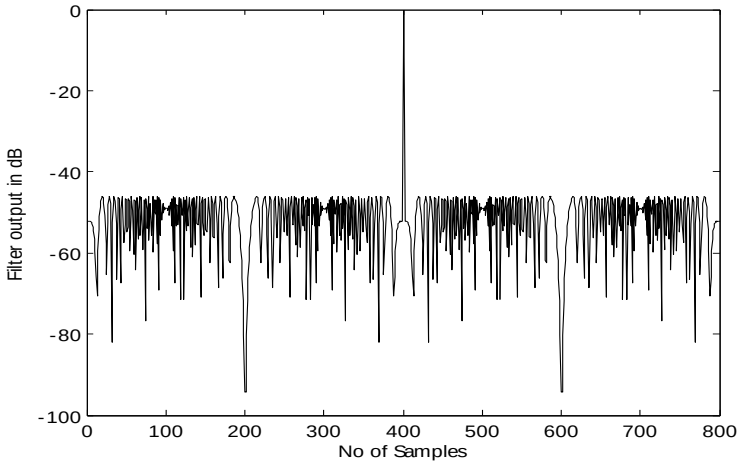

Figure 3.10 Result of sliding window two-sample adder on output of 400 to1 P4 code

The effect of double TSSWA and TSSWS is show in Fig 3.10

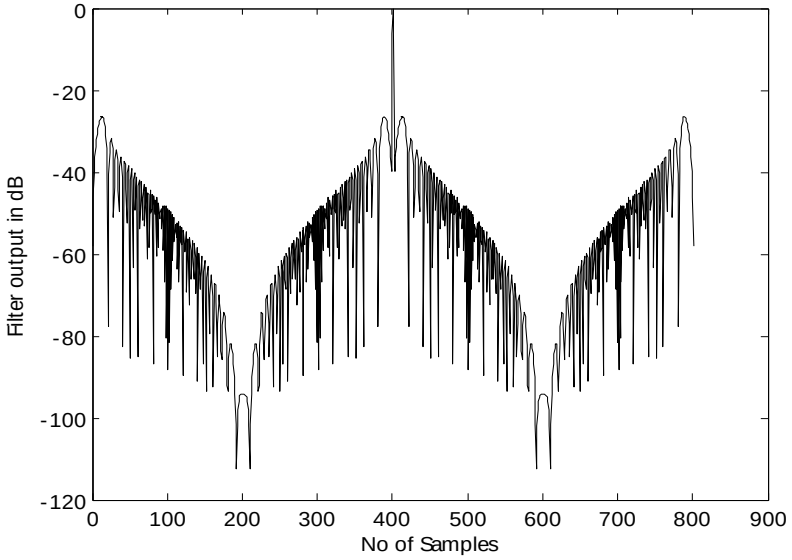

(a)

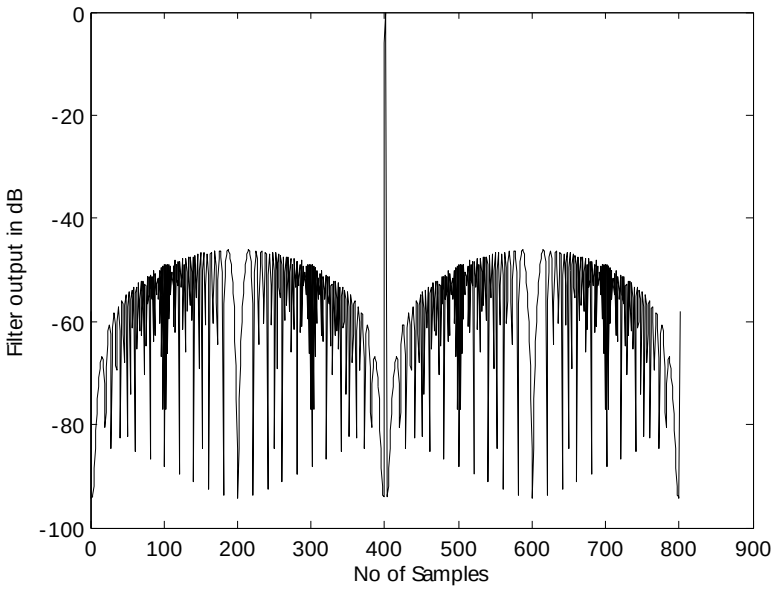

(b)

Figure 3.11. 400-element P4 code (a) Double TSSWA output after autocorrelator (b) Double TSSWS output after autocorrelator

3.4.2 Effect of Doppler on TSSWA

Tests of the sidelobe suppressor with Doppler such as would be encountered in radar where the codes were useful revealed that the Doppler did not significantly reduce the effect of the sidelobes suppressor. Figure 3.11 illustrates the effect of a Doppler shift *f* to signal bandwidth B ratio *f*/B = 0.01.

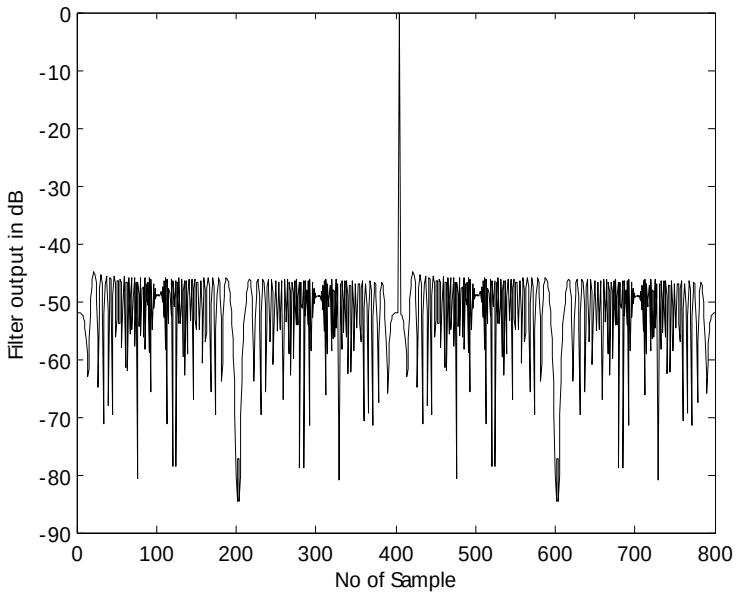

Figure 3.12 Result of sliding window two-sample adder on output of 400 to 1 P4 code compressor with 0.01 *f*/B Doppler shift

The shift of the signal peak 4 range resolution cells to the left. This range Doppler coupling is characteristics of frequency or frequency derived polyphase coded pulse compression waveforms.

3.4.2 Price paid for sidelobe reduction

The sliding window circuits shown in Fig 3.7 and 3.9 reduced the sidelobes but also doubled the width of the mainlobe .Thus, the effective pulse compression ratio is only 200 to 1 while the reciprocal of the signal bandwidth is still 400 times smaller than the reciprocal of the transmitted pulse length. In this process of doubling the compressed pulse length, the sliding window two-sample adder doubled the thermal noise power without changing the signal power.

It should be noted that this signal-to-noise having in each time element T does not reduce the signal detectability by 3dB since the bandwidth was not halved at the same time if digital compressors were used. Actually a detector would have two chances to detect the signal in two adjacent time cells containing different noise values. As a consequence, the sidelobe reduction would only cost a signal-to-noise ratio loss on the order of 1dB [3.2].

It should also be noted that the observed 46dB sidelobe levels in Figs 3.7 and 3.9 are only one code element magnitude in a pulse compression ratio of 200 to 1 system. Thus the two-sample sliding window subtractor in the output of a digital Frank or P1 code compressor can limit the compressed pulse range-time-sidelobes to those of the Barker codes with unlimited pulse compression ratios.Also it demonstrated that a two-sample sliding window adder would do the same thing for the P3 and P4 polyphase codes. The significant sidelobe reduction would only cost on the order of 1dB loss in signal-to-noise ratio.

3.5 Weighting Techniques for Polyphase Codes

There will be significant reduction in sidelobes and PSL values than TSSWA by implementing time weighting function to the signal code. This sidelobe reduction technique can be analyzed in two ways, one is matched weighting with weighting window at the transmitter and the receiver and two is mismatched weighting, where amplitude weighting is performed only at receiver site [3.4]. In this section, simulations are done using mismatched weighting. The tradeoff in reducing the PSL is a spreading of the peak value of the compressed pulse, or mathematically the autocorrelation (ACF) function, resulting in a loss in resolution similar to that of a chirp waveform. The greater the amplitude taper, for example a cos^n weighting as n is raised to a higher power, the narrower the bandwidth and hence the wider the compressed pulse. Also**,** there is a loss in s/n similar to the weighted chirp waveform. Good Doppler tolerance is maintained with these weightings, especially with the Taylor weighting. However, in contrast the sidelobes decrease as the number of P4 code elements increase.

In this section, Kaiser-Bessel time weighting function is analysed due to β parameter and its influence on sidelobe suppression and efficiency in Doppler shift domain, as well. The PSL and integrated sidelobe level (ISL) values are compared for different weighting functions such as Kaiser-Bessel, hamming, hanning, Blackman etc.

3.5.1. Hamming Window

Hamming window belongs to the family of raised cosine windows. The window is optimized to minimize the maximum (nearest) side lobe, giving it a height of about one-fifth that of the Hann window, a raised cosine with simpler coefficients. The coefficients of a Hamming window are computed from the following equation[3.6].

$$w(n) = 0.54 - 0.46\cos\left(2\pi\frac{n}{N}\right), \quad 0 \le n \le N \tag{3.7}$$

The 100- point hamming code is shown in Figure 3.12.

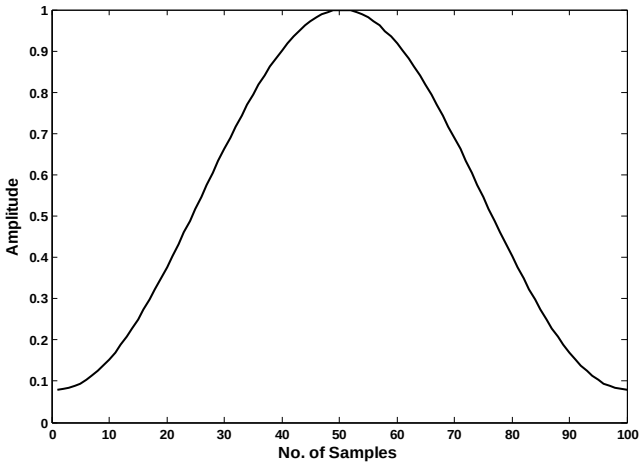

Figure 3.13 Hamming code of length 100

3.5.2. Rectangular Window

The rectangular window is sometimes known as a Dirichlet window. It is the simplest window, taking a chunk of the signal without any other modification at all, which leads to discontinuities at the endpoints (unless the signal happens to be an exact fit for the window length, as used in multitone testing, for instance).[3.7] The first side-lobe is only 13 dB lower than the main lobe, with the rest falling off at about 6 dB per octave.

$$W(n) = 1 \tag{3.8}$$

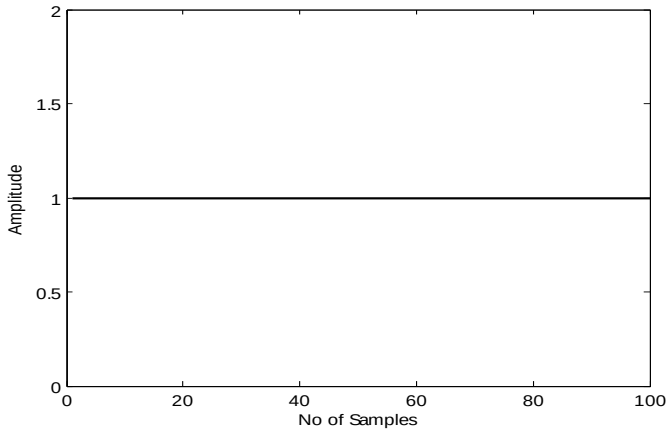

Figure 3.14 Rectwindow code of length 100

3.5.3. Hann Window

The Hann and Hamming windows, both of which are in the family known as "raised cosine" windows, are respectively named after Julius von Hann and Richard Hamming. The term "Hanning window" is sometimes used to refer to the Hann window [3.6, 3.7]. While the Hanning window does a good job of forcing the ends to zero, it also adds distortion to the wave form being analyzed in the form of amplitude modulation; i.e., the variation in amplitude of the signal over the time record. Amplitude Modulation in a wave form results in sidebands in its spectrum, and in the case of the Hanning window, these sidebands, or side lobes as they are called, effectively reduce the frequency resolution of the analyzer by 50%. The advantage of the Hann window is very low aliasing, and the tradeoff is slightly decreased resolution (widening of the main lobe).

The coefficients of a Hann window are computed from the following equation.

$$w(n) = 0.5\left(1 + cos\left(\frac{2\pi n}{N-1}\right)\right) \tag{3.9}$$

or $$w(n) = sin^2\left(\frac{\pi n}{N-1}\right)$$

The window length is L=N+1

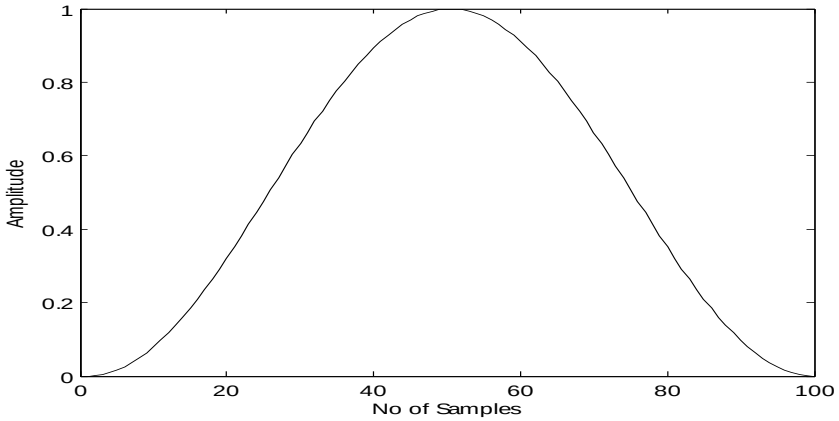

Figure 3.15 Hanning code of length 100

3.5.4. Blackman Window

The Blackman window is quite similar to Hann and Hamming window, but it has one additional cosine term to further reduce the ripple ratio. Blackman windows have slightly wider central lobes and less sideband leakage than equivalent length Hamming and Hann windows.

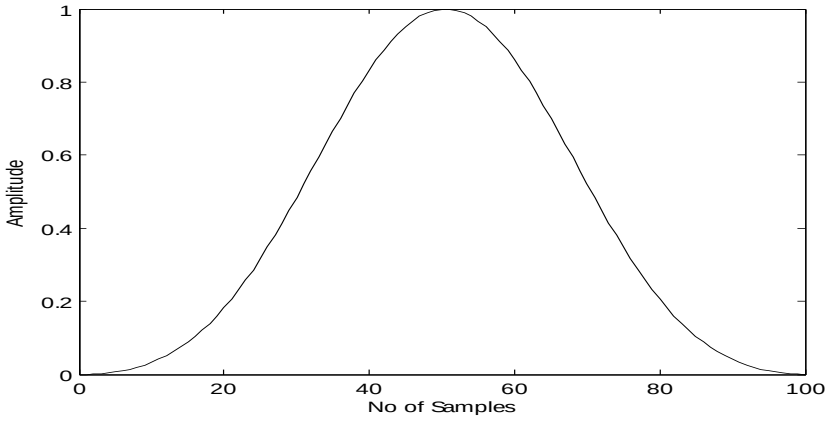

Figure 3.16 Blackman code of length 100

The coefficients of a Hann window are computed from the following equation

$$w(n) = a_0 - a_1 cos\left(\frac{2\pi n}{N-1}\right) + a_2 cos\left(\frac{4\pi n}{N-1}\right) \qquad (3.10)$$

$$a_0 = \frac{1-\beta}{2}, a_1 = \frac{1}{2}, a_2 = \frac{\beta}{2}$$

By common convention, the unqualified term *Blackman window* refers to α=0.16.

3.5.5. Kaiser-Bessel Window

For a Kaiser-Bessel window of a particular length N, the parameter β controls the sidelobe height and it affects the sidelobe attenuation of the Fourier transform of the window. This parameter also trades off main lobe width against side lobe attenuation[3.8]. The Kaiser-Bessel window in sampled version with β is computed as follows

$$w[n] = \begin{cases} \dfrac{I_0\left(\beta\sqrt{1-\left(\dfrac{2n}{N-1}-1\right)^2}\right)}{I_0(\beta)}, & if \quad 1 \le n \le N \\ 0, otherwise \end{cases} \tag{3.11}$$

Where I_0 is the $Zero^{th}$ order modified Bessel function of the first kind, β is an arbitrary real number that determines the shape of the window, N is the length of the window. The design formula that is used to calculate β parameter value due required a sidelobe level

$$\beta = \begin{cases} 0.1102(\alpha - 8.7), & \alpha > 50 \\ 0.5842(\alpha - 21)^{0.4} + 0.07886(\alpha - 21), & 21 \le \alpha \le 50 \\ 0, & \alpha < 21 \end{cases} \tag{3.12}$$

Where α is sidelobe level in decibels. As β increases, the main lobe width widens and the sidelobe attenuation increases. For β = 0, the Kaiser-Bessel window is a rectangular window. For β= 5.44, the Kaiser-Bessel window is close to the Hamming window. Typically, the value of β is in the range from four to eight and for a given parameter, the sidelobe height is fixed with respect to window length [3.7, 3.8].

The Kaiser-Bessel window of length 100 for different values of β is plotted in Figure 3.16.

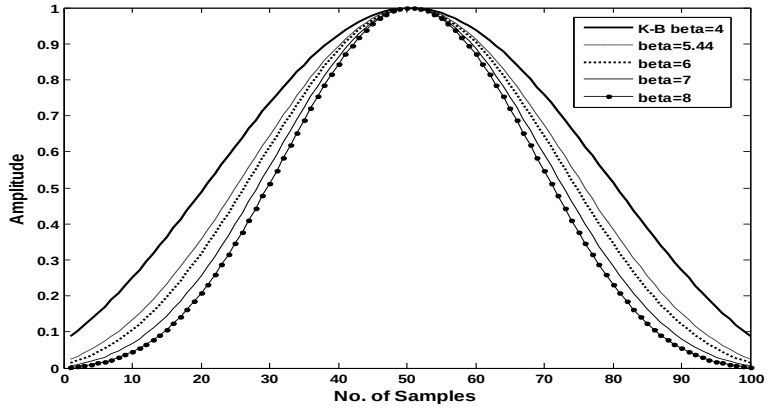

Figure 3.17 Kaiser-Bessel code of length 100 for different β values

For any given window, the signal-to-noise loss (SNR loss) can be calculated by the formula

$$SNR_{loss} = \frac{\left(\sum_{n=1}^{N} w[n]\right)^2}{\sum_{n=1}^{N} w[n]^2} \tag{3.13}$$

3.5.6. Simulation Results and Discussion

All window functions discussed above are applied as sidelobe reduction techniques for P4 code.

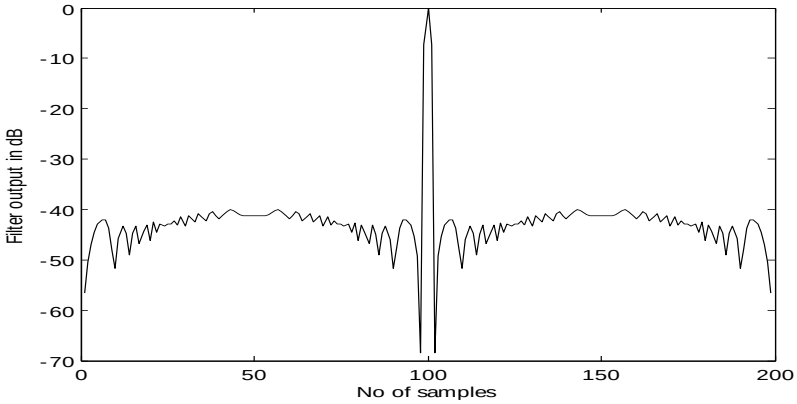

Figure 3.18 ACF of P4 100 with hamming window

At the receiver side, the code signal is multiplied with the window coefficients and the weighted code and transmitted one are subjected to autocorrelation.

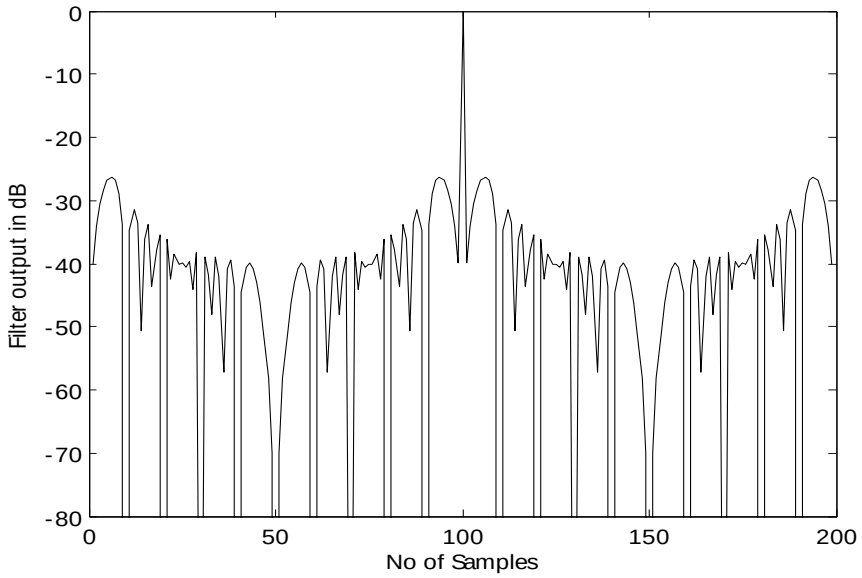

Figure 3.19 ACF of P4 100 with Rectangular window

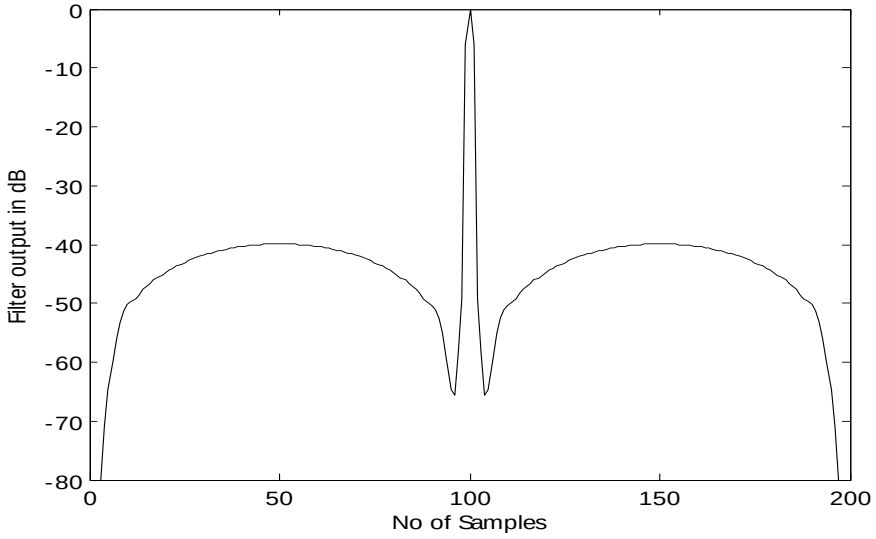

Figure 3.20 ACF of P4 100 with Hann window

The autocorrelated output using Kaiser Bessel window for different values of β for P4 code of length 100 is given in Figure 3.20.

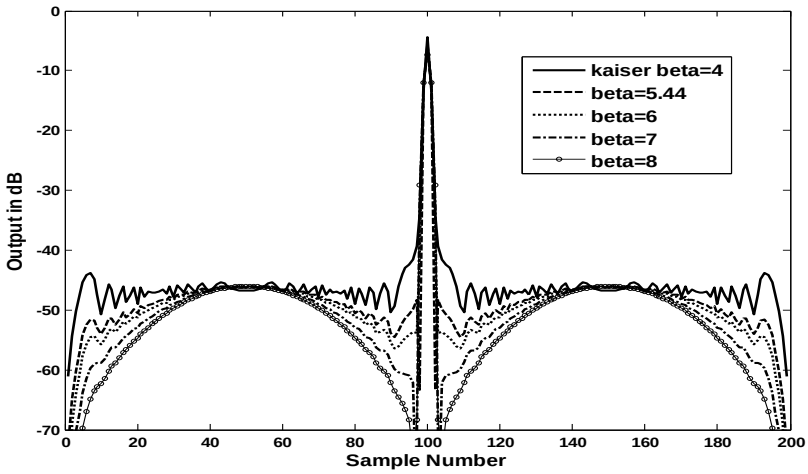

Figure 3.21. Autocorrelation function of P4 signal, N=100, Kaiser-Bessel window for various β parameter value

Table 3.1. Performance for 100 element P4 code

Window name	Peak Sidelobe Level (dB)	Integrated Sidelobe Level (dB)	Weighting SNR loss
Rectangular	26.32	12.00	0
Hamming	40.08	19.73	1.37
Hanning	39.9	21.8	1.73
Blackman	38.4	22.24	1.43
Kaiser-Bessel β=4	29.78	18.29	0.98
K-B, β=5.44	40.34	19.29	1.52
K-B, β=6	35.06	19.72	1.71
K-B, β=7	26.19	18.28	1.99
K-B, β=8	21.77	16.28	2.26

By comparing the above results Kaiser-Bessel with β=5.44 gives better PSL and ISL than all other windows applied

3.6. Doppler Properties of P4 weighted Code

The effect of amplitude weighting of Hamming and Kaiser Bessel windows of P4 code under Doppler shift conditions are examined [3.2]. Figure 3.21(a) shows the ACF of P4 signal for various Doppler shifts, where the one is normalized to the signal bandwidth. Figure 3.21(b) shows the effects of Hamming and Kaiser Bessel windowing techniques under Doppler of -0.05. The PSL and ISL values under Doppler of -0.05 for weighed P4 code are depicted in Table 3.3.

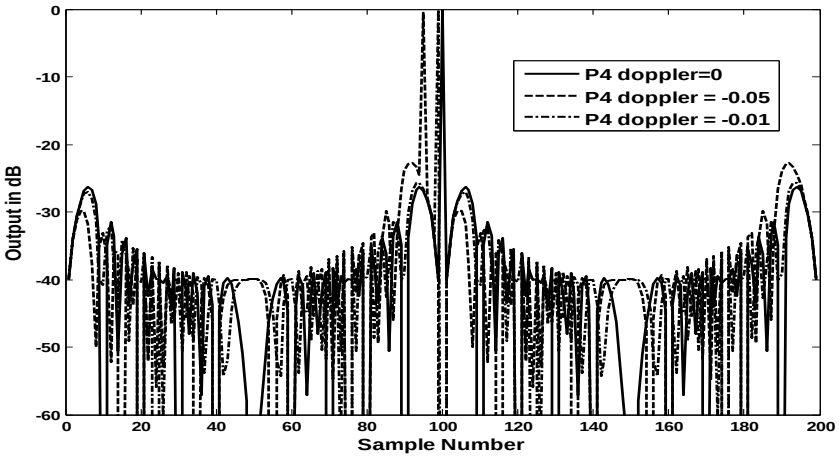

(a)

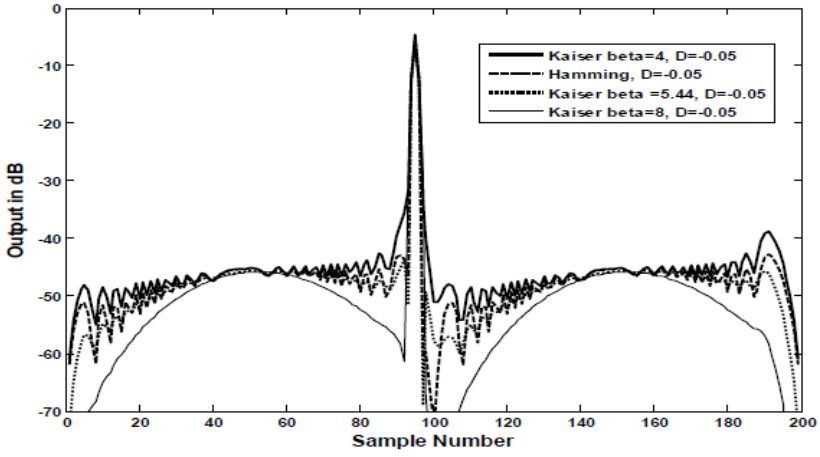

(b)

Figure 3.22. Autocorrelation function of 100-elementP4 signal (a) weighted P4 code (b) for various windows and Doppler shift of -0.05

Table 3.2. Performance for 100 element P4 code under Doppler shift of -0.05

Window name	Peak Sidelobe Level (dB)	Integrated Sidelobe Level (dB)
Rectangular	-22.38	-10.66
Hamming	-37.29	-19.01
Kaiser-Bessel β=4	-27.14	-17.35
K-B, β=5.44	-37.98	-19.38
K-B, β=8	-21.78	-16.21

3.7. Summary

A detailed structure of sidelobes is discussed and different sidelobe reductions techniques such as Single TSSWA and double TSSWA outputs for P4 code are explained in detail and proved that this technique reduces the PSL value. In order to reduce the PSL values further, weighting techniques are employed. The Hamming and Kaiser Bessel windowing functions are studied and their effects to P4 code under Doppler of 0 and -0.05 are discussed.

Chapter 4

WOO Filter sidelobe reduction technique for pulse compression

4.1 Introduction to woo filter

A uniform sidelobe level represents an optimum performance criterion in the design of pulse compression waveforms .This chapter describes a new form of pulse compression filter for polyphase codes is presented which generates a flat uniform sidelobe pattern similar to those obtainable from Barker codes. The sidelobes levels are decided solely by the length of the phase codes, which can be set arbitrarily [4.1]. Their use involves a small loss and degradation in range resolution, but excellent Doppler tolerance. Phase coded waveforms tend to be favored when low sidelobes levels are desired. In addition compatibility with digital generation and compression makes their use more attractive. Barker codes are known to give good performance; they achieve unit peak sidelobes level throughout the entire sidelobe regions, which is why they are known as 'perfect' codes. However, their limited code length and high Doppler shift sensitivity restrict their applications.

Lewis argued that the adjacent cells within the P3 and P4 autocorrelation outputs differ in magnitude by no more than the magnitude of one element cell [4.2]. This assertion was made intuitively on the ground that an additional input into the matched filter cannot cause variations of more than its own magnitude at the output. The time range sidelobes reduction scheme introduced by Lewis can be interpreted as a pulse compression on P codes by use of combination of two separate correlation filters. Thus a new type of compression filter is needed to achieve this optimal uniform sidelobes which is explained in this chapter.

4.2 Implementation of woo filter

Let S (t) is a polyphase code sequence directly derived from a conventional linear FM signal [4.4]. The function S (t) may be expressed as

$$S(t) = \sum_{p=0}^{N} \exp\left(j\frac{\pi}{N}p^2\right) U\left[\frac{t-(p+\frac{1}{2})t_b}{t_b}\right] \qquad (4.1)$$

Where $U(t) = 1$ for $|t| \leq \frac{1}{2}$ and Zero elsewhere, t_b is the time duration of one element of the codes sequences. Basically S (t) is identical to the P3 code apart from a new term added at the end of the sequence to make it perfectly symmetrical [4.3]. When the pulse compression ratio is

sufficiently high, it can be shown that the amplitude difference adjacent values in the autocorrelation output fluctuate according to a specific function that eventually converges to

$$2cos\left[\frac{\pi}{N}(p-1)^2\right] \tag{4.2}$$

Instead of carrying out subtraction after pulse compression, two identical sequences, but shifted by 1-bit, can be incorporated into the correlation filter to obtain this magnitude difference curve directly. With this approximate formulation in mind, a direct way to achieve ideal unit amplitude sidelobes pattern can be implemented [4.6].

Let S (p) be a representation of the signal S (t).

Then the *qth* term in the first sidelobe part $(1 < q \leq N)$of the autocorrelation output can be designed as

$$\Omega_1(q) = \sum_{p=0}^{q=1} s(p)^*.s(N-q+p+1) \tag{4.3}$$

When N even terms are taken the first term in the equation becomes

$$s(N-q+p+1) = s(q-1) = \exp\left(j\frac{\pi}{N}(q-1)^2\right) \tag{4.4}$$

Let the equation (4.3) is produced by one of the sequence inside the composite correlation filter. Now by comparing this result with the sidelobe reduction term show in equation (4.2),it be observed that by removing the first term in the equation(4.4) during the composite correlation procedure the output which can be obtained at of the correlation filter is given by

$$2cos\left[\frac{\pi}{N}(p-1)^2\right] - \exp\left(j\frac{\pi}{N}(q-1)^2\right) = \exp\left(-j\frac{\pi}{N}(q-1)^2\right) \tag{4.5}$$

By implementing the above procedure the sidelobes levels are maintained at unity. To put this into practice another correlation filter as shown in equation (4.6) should be considered.

$$\Omega_2(q) = \sum_{p=0}^{q=1} s(p)^*.s(N-q+p) \tag{4.6}$$

For $(1 < q \leq N)$should be considered

The function $\Omega_2(q)$ is one bit shifted version of $\Omega_1(q)$ with its first term removed and a new term added at the end. Under the assumption of a reasonable high pulse compression ratio

$N = BT$, and for values of q relatively large compared to unity but not very close to N, the difference between $\Omega_2(q) - \Omega_1(q)$ approximates exp (-j (π/N)q^2).

Since there is a linear relationship between $\Omega_1(q)$ and $\Omega_2(q)$, and since each function is composed of same number of terms these correlations filters fuse for generating $\Omega_1(q)$ and $\Omega_2(q)$ can be combined to produce a new discrete filter *W(p)* which denote the Woo filter. The phase coded signal and Woo filter have similar structure so identical structure can be obtained at other sidelobe regions. The amplitude variation in the time domain indicates that the Woo filter results from a parabolic complex weighting of the original signal.

4.2.1 Mathematical derivation of new phase code

Consider a polyphase sequence S (t) having $(N + 1)$elements

$$S(t) = \sum_{p=0}^{N} \exp\left(j\frac{\pi}{N}p^2\right) U\left[\frac{t-(p+\frac{1}{2})t_b}{t_b}\right] \tag{4.7}$$

Where $U(t)$ =1 for $|t| < \frac{1}{2}$ and Zero elsewhere. t_b Be the time duration of one element in the codes sequences. Let $s(p)_{s-p3}(p = 0 \ldots N)$, When will be denoted as $s - P3$, be the discrete form of $S(t)$:

$$s(p)_{s-p3} = \sum_{p=0}^{N} \exp\left(j\frac{\pi}{N}p^2\right) \tag{4.8}$$

$s(p)_{s-p3}$ is identical to the P3 code except that a Zero phase term is added at the beginning of the sequence to make the sequenced symmetric, which is useful in reducing calculation complexity for deriving the ACF[4.10].

Let the *qth* term of correlation filter output for the $s - P3$ code be designated by equation (4.3) the *qth* term of the equation can be shown by

$$\Omega_1(q) = (-1)^N \frac{sin\left[\frac{\pi}{N}q(q-1)\right]}{sin\left[\frac{\pi}{N}(q-1)\right]} \tag{4.9}$$

The difference between the two adjacent terms is given by

$$\Omega_1(q+1) - \Omega_1(q) = (-1)^N \frac{sin\left[\frac{\pi}{N} q(q+1)\right]}{sin\left[\frac{\pi}{N}(q)\right]} - \frac{sin\left[\frac{\pi}{N} q(q-1)\right]}{sin\left[\frac{\pi}{N}(q-1)\right]} \tag{4.10}$$

$$= \frac{sin\left[\frac{\pi}{N} q(q-1)\right] sin\left[\frac{\pi}{N} q(q+1)\right] - sin\left[\frac{\pi}{N} q(q-1)\right] sin\left[\frac{\pi}{N}(q)\right]}{sin\left[\frac{\pi}{N}(q)\right] sin\left[\frac{\pi}{N} q(q-1)\right]}$$

$$= cos\left(\frac{\pi}{N}(q^2+1)\right) - cos\left(\frac{\pi}{N}(q^2-2q-1)\right)$$

$$= \frac{cos\left(\frac{\pi}{N}(q^2-2q)\right) - cos\left(\frac{\pi}{N}(q^2)\right)}{cos\left(\frac{\pi}{N}\right) - cos\left(\frac{\pi}{N}(2q)\right)}$$

$$= cos\left(\frac{\pi}{N}(q^2)\right) - cos\left(\frac{\pi}{N}(q^2+2q)\right) - cos\left(\frac{\pi}{N}(q^2-2q)\right) - cos\left(\frac{\pi}{N}(q^2)\right)$$

$$= \frac{2cos\left(\frac{\pi}{N}(q^2)\right) - 2cos\left(\frac{\pi}{N}(q^2)\right).cos\left(\frac{\pi}{N}(2q)\right)}{sin\left(\frac{\pi}{N}(q)\right) sin\left(\frac{\pi}{N}(q-1)\right)}$$

$$= (-1)^N 2cos\left(\frac{\pi}{N}(q^2)\right) \tag{4.11}$$

This is still a function of magnitude 2, but expressed in a simpler form compared with the non-symmetrical P3 case. The first term of this summation equation is given as $S(0).S(N-q-1)$ and is equal to$\exp\left(\frac{\pi}{N}(q-1)^2\right)$. Here only even values of N will be considered for convince, although exactly the same result but with opposite sign will be obtained for the case of odd N. By observing the result with equation (4.11) it can be observed that by removal of the first term in the equation (4.9) the ranges sidelobe will be kept at unity [4.6, 4.10].

This is show in the following mathematical derivation

$$\Omega_1(q) = (-1)^N \frac{sin\left[\frac{\pi}{N} q(q-1)\right]}{sin\left[\frac{\pi}{N}(q-1)\right]} \tag{4.12}$$

Now by removing the first term to make it unit magnitude

$$\Omega_1(q) - \exp\left(\frac{\pi}{N}(q-1)^2\right) - \Omega_1(q-1)$$

$$= 2cos\left(\frac{\pi}{N}(q^2)\right) - \exp\left(\frac{\pi}{N}(q-1)^2\right)$$

$$= \exp\left(-\frac{\pi}{N}(q-1)^2\right)$$

$$\Omega_2(q) = \sum_{p=1}^{q} s(p)^*.s(N-q+p)$$

$$\Omega_2(q) - \Omega_1(q) = cos\left(\frac{\pi}{N}(q^2)\right) - jsin\left(\frac{\pi}{N}(q^2)\right)$$

$$= \exp\left(-\frac{\pi}{N}(q-1)^2\right) \quad (4.13)$$

Thus equation (4.13) shows range sidelobe is kept unity by first term from the second Correlator.

4.2.2 Correlator development and implementation

Previous section includes some approximations on correlation function, their exact formulation are pursued to validate our claims. The *qth* term of Correlator output $\Omega_1(q)$ is calculated as

$$\Omega_1(q) = \sum_{p=0}^{q-1} \exp\left(-j\frac{\pi}{N}p^2\right).\exp\left(j\frac{\pi}{N}\left({\delta_1}^2 + 2\delta_1 p + p^2\right)\right) \quad (4.14)$$

$$= \exp\left(j\frac{\pi}{N}(\delta)^2\right).\sum_{p=0}^{q-1}\exp\left(j\frac{\pi}{N}2\delta_1 p\right) \quad (4.15)$$

Where $\delta_1 = N - q - 1$

A similar procedure is carried for the other Correlator $\Omega_2(q)$.

$$\Omega_2(q) = \sum_{p=0}^{q-1} \exp\left(-j\frac{\pi}{N}p^2\right).\exp\left(j\frac{\pi}{N}\left({\delta_2}^2 + 2\delta_2 p + p^2\right)\right) \quad (4.16)$$

Where $\delta_2 = N - q$

After computing the geometric sequence summation, it is shown that each $\Omega_1(q)$ and $\Omega_2(q)$ are shown in the following equations.

$$\Omega_1(q) = (-1)^N \frac{sin\left[\frac{\pi}{N} q(q-1)\right]}{sin\left[\frac{\pi}{N}(q-1)\right]} \tag{4.17}$$

$$\Omega_2(q) = (-1)^N \exp\left(-j\frac{\pi}{N} q\right) \frac{sin\left[\frac{\pi}{N} q^2\right]}{sin\left[\frac{\pi}{N} q\right]} \tag{4.18}$$

Since the Correlators that generate $\Omega_1(q)$ and $\Omega_2(q)$ are of the same length, they can be combined to become a new single filter $W(p)$ be denoted as the woo filter for convenieced.Then the woo filter for the $s-P3$ code,$Woo_{s-P3}(t)$, it is described in the time domain as

$$Woo_{s-P3}(t) = \sum_{p=1}^{N} \left\{ \exp\left(-j\frac{\pi}{N}(p)^2\right) - \exp\left(-j\frac{\pi}{N}(p-1)^2\right).U\left[\frac{t-(p-\frac{1}{2})t_b}{t_b}\right]\right\}$$

$$= \sum_{p=1}^{N} \left\{ 2\text{jsin}\left(\frac{\pi}{N}(p-1/2\right) - \exp\left(-j\frac{\pi}{N}(p^2+p-1/2\right).U\left[\frac{t-(p-\frac{1}{2})t_b}{t_b}\right]\right\} \tag{4.19}$$

Let $Woo(n)$ be a discrete form converted from $woo(t)$.After substituting equations (4.17) and (4.18) into (4.13), the correlation between $Woo_{s-P3}(n)$ and the $s-P3$ codes results in

$$Woo_{s-P3}(n) \otimes S_{p3}(n') \cong (-1)^N \exp\left(-j\frac{\pi}{N} q^2\right) \tag{4.20}$$

A similar procedure can be applied to the s-P4 code. Figure 4.1 shows the magnitude and phase angle distribution of the woo filter along the time axis. The amplitude envelopes of the woo filter are equivalent to weighting function that reduces low frequency components for the s-P3 [4.9].

This pulse compression technique form the conventional technique is inherently distinguished from the conventional weighting methods such a Hann, Ham or Dolph-Chevyshev which are discussed the previous chapter in which both the magnitude and phase are affected at the receiving Correlator.

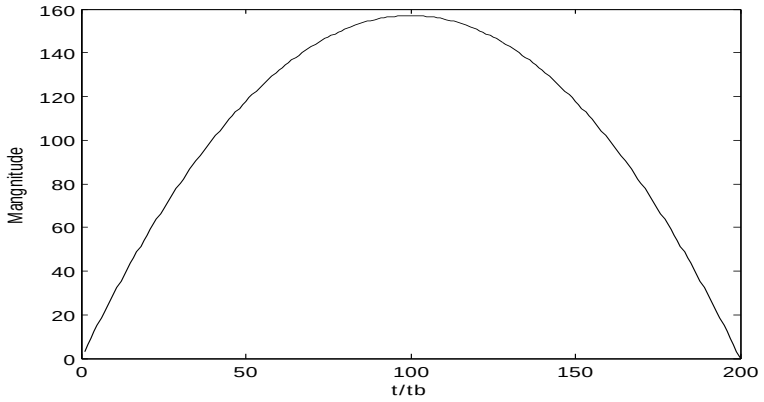

(a)

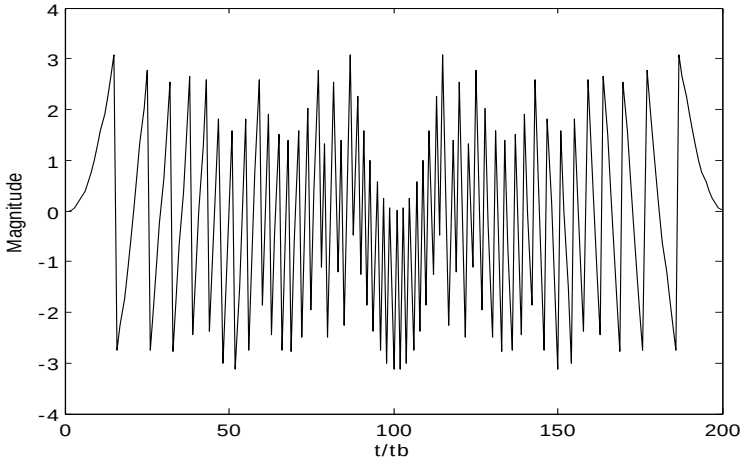

(b)

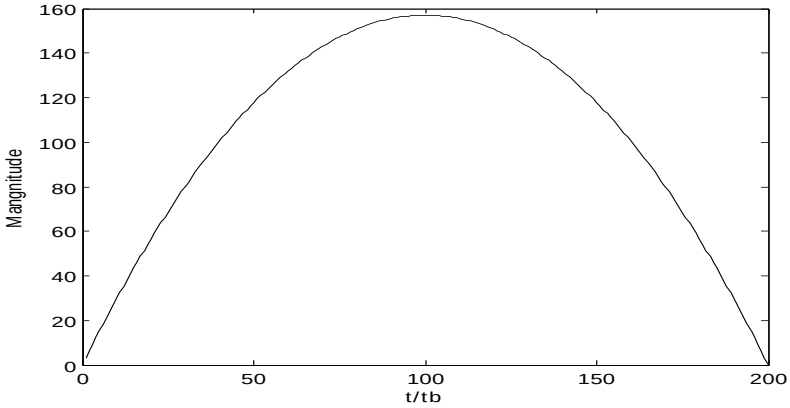

(c)

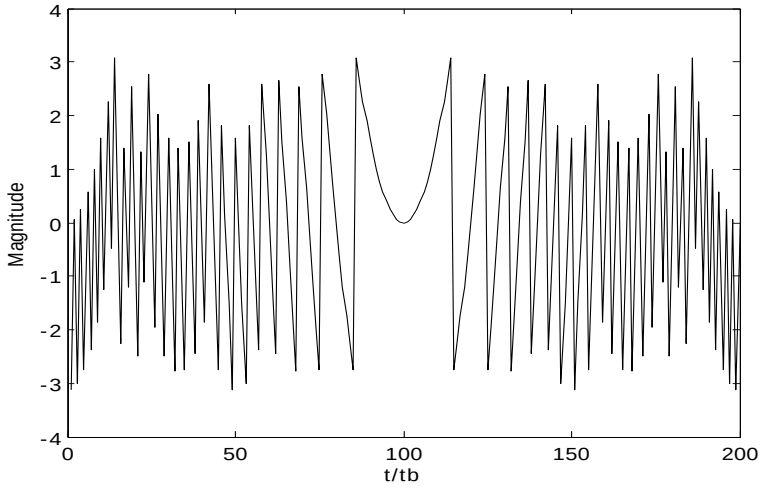

(d)

Figure4.1 Amplitude and phase angle variations along time axis of Woo filter

4.2.3 Range sidelobe performance analysis

Figure4.2 shows illustrates the pulse compression outputs when the Woo filter is used as a Correlator. The signal consists of 200 and 1000 sub- pulses each of length t_b while their corresponding Woo filter have 199 and 999 elements respectively. As predicted, uniform sidelobe pattern has been achieved throughout the entire time range bins except at the beginnings and ends of the sidelobes sequences [4.10].

The uniform sidelobes, which is decided solely by the signal code length, is kept at a constant level consistently over whole sidelobe ranges. Apart from our ripple peaks that appear at both ends of the sidelobes, the uniform levels, which now can be considered as the PSL, are -46dB and -60dB respectively. These exactly correspond to $20log_{10}(200)$ and$20log_{10}(1000)$, the Barker code level for these signal codes lengths. The existence of the ripples can be predicted from the equation (4.20), which is assumed to work only for large q values.

Another important property to reduce is the complete isolation of the mainlobe by the extremely low sidelobe level around it, which gives rise to a mainlobe sharpening effect. This is due to the fact that, for a small q , the two separate summations of the correlation fitlers have nearly identical values[4.7]. The expressions of the two Correlator shows that as N increases, the values converge to each other and the mainlobe isolation distance is widened this isolation distance

increases linearly in proportion of the pulse code length$N$. Because the Woo filter is one bit shorter than the incoming signal and its structure is symmetrical in the time domain, the mainlobe width is broadened by a factor of two. This can be understood as a fraction of the signal power in the sidelobe being pushed towards the mainlobe area by the Woo filter.

The increased mainlobe width may easily be compensated by increasing the signal bandwidth or imposing a non-symmetric weighting on the Correlator [4.10].

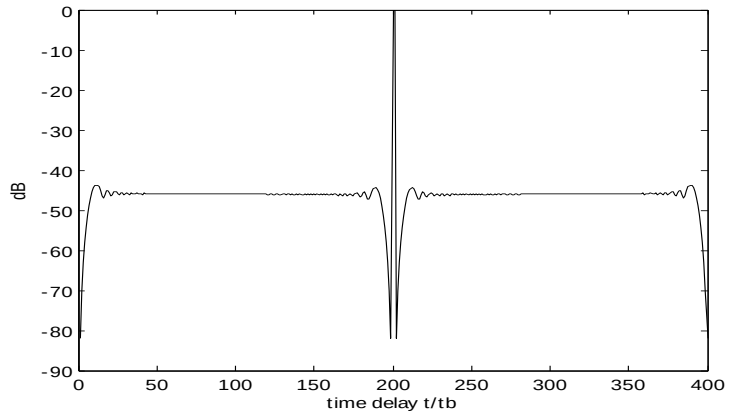

(a)

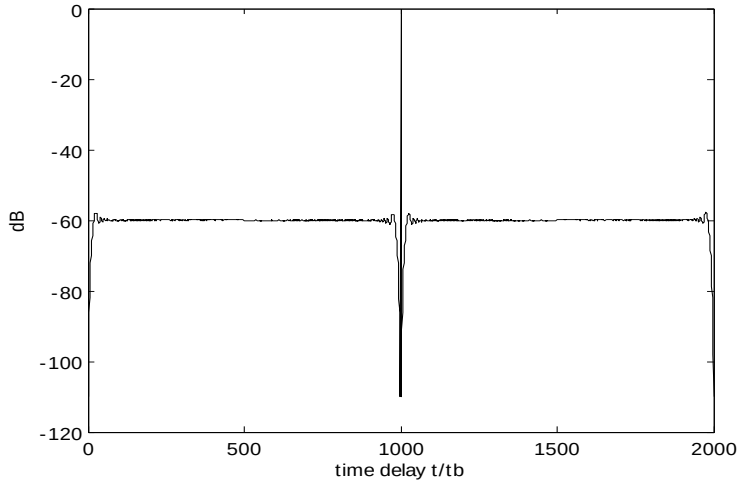

(b)

Figure 4.2. S-P4 code pulse compression outputs by Woo filters for code length N=200 and 1000

(a) N=200 and (b) N=1000.

4.2.4 Doppler shift effect

The pulse compression response of Woo filter corresponding to various Doppler frequency shifted signals are shown in Figure 4.3. This Woo filter is considered as a linear combination of matched filters for linear FM derived phase codes. Therefore it would be logical to anticipate that its response would be similar to that of linear FM.[4.10] Some distinctive characteristics are found concerning the mainlobe, ripple peaks and range direction shift.

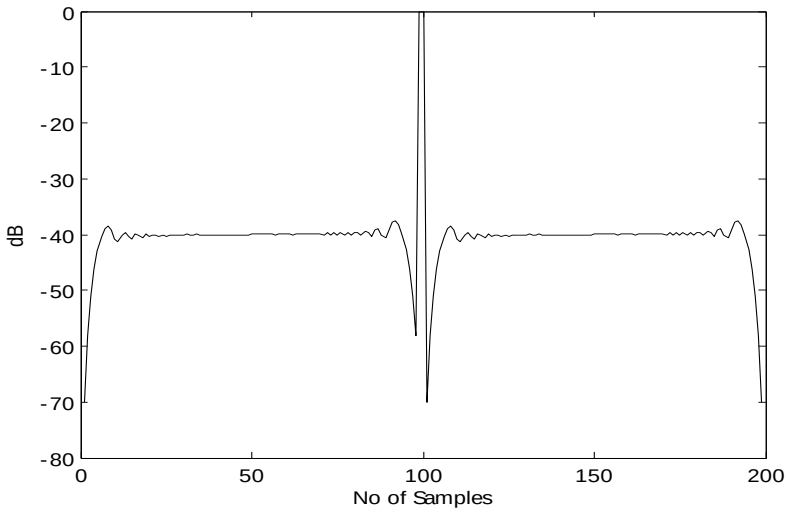

(a)

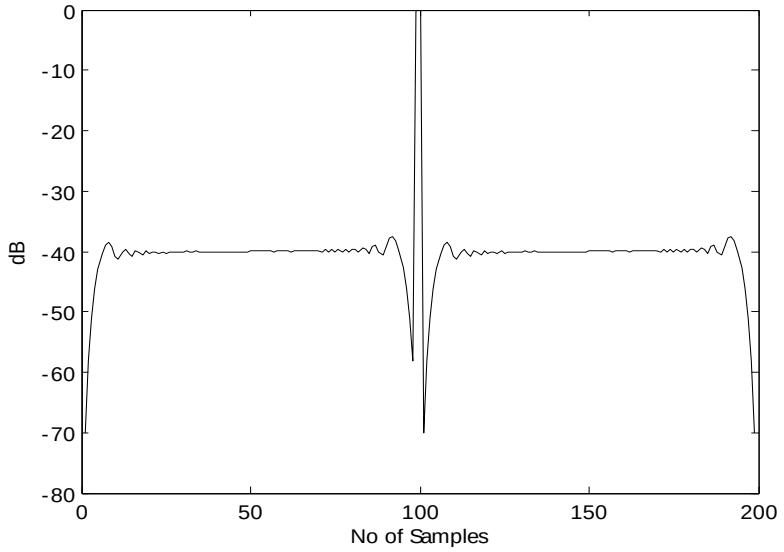

(b)

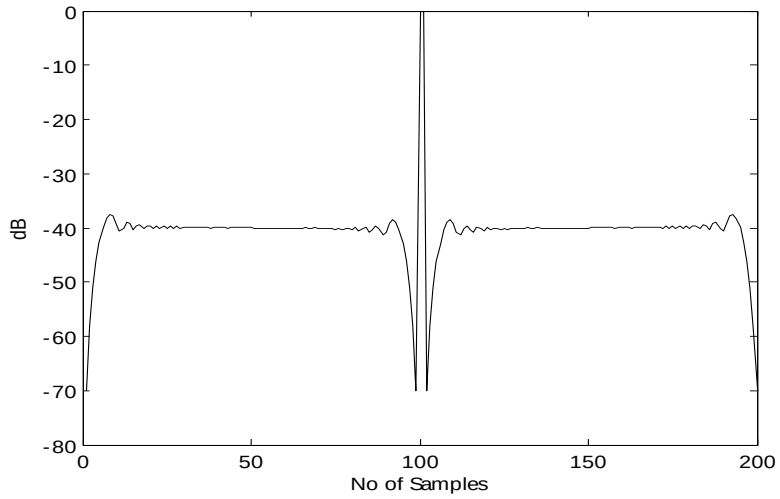

(c)

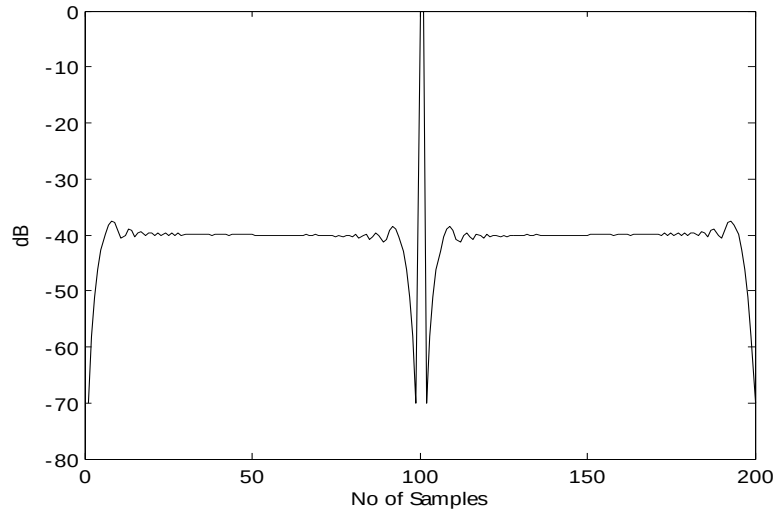

(d)

Figure 4.3 Woo filter outputs of Doppler shifted signals with Doppler shifts of 1, 2,3and 4% of the signal bandwidthB_d. Pulse code length N=100

(a) f_d=1% (b) f_d=2% (c) f_d=3% (d) f_d=4%

The peak ripples (PR) appearing at the edge of the sidelobe also changes according to the frequency shift. The sidelobe also at both sides behave in a symmetrical way.

4.3 Modified Woo filter

The modified version proposed Woo filter is formulated by adopting post compression processing. This way Woo filter is restructured which is shown in Figs.4.4 and 4.5. This overcomes the mainlobe splitting which is the major disadvantage in original Woo filter. In form-I one bit shifted version of the input code is combined with two bit shifted version and later the combined output signal is subjected to correlation. This structure is shown in Fig.4.4 as form-I. In form I, Two bit shifted p4 signal is considered as the received signal expecting one bit delay in transmitting and receiving process. One bit shifted p4 signal is transmitted and the same is considered as the reference signal. The reference signal is added to the received signal and then correlated. In the form-II the signal is combined with one -bit shifted version of itself and the resulting signal is passed through correlation process. This structure is shown in Fig.4.5 as form-II. In this form II, One bit shifted p4 signal is considered as the received signal expecting one bit delay in transmitting and receiving process [4.8].

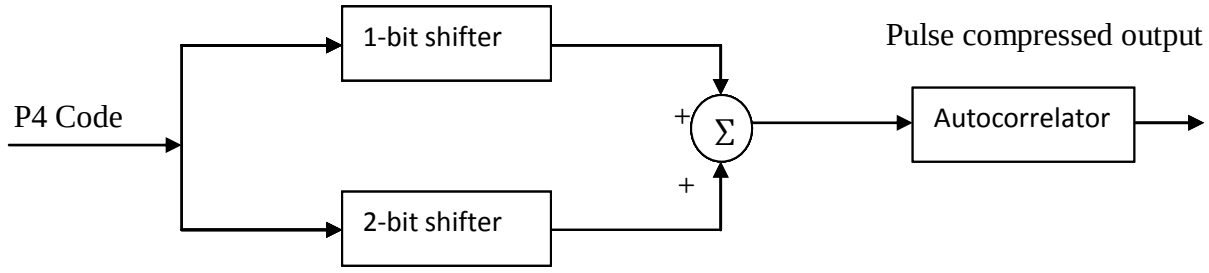

Figure 4.4 A schematic diagram of sidelobe reduction using modified Woo filter form-I.

P4 signal is transmitted and the same is considered as the reference signal at the receiver. The reference signal is added to the received signal and then correlated. Here matched filter is used as the Autocorrelator. In both the forms, PSL and ISL values are much higher than original Woo filter. We observed that form I produces uniform sidelobes.

However PSL and ISL levels of form I and form II are same. PSL and ISL are reduced significantly and Doppler tolerance is improved but increases the mainlobe width. Mismatch loss and SNR loss are not affected by this new scheme.

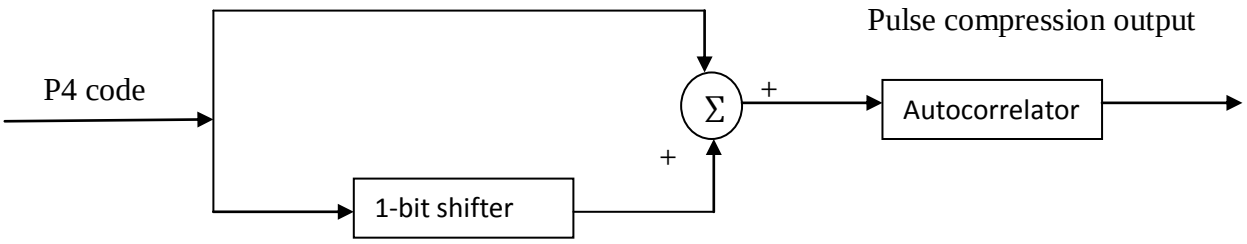

Figure 4.5 A schematic diagram of sidelobe reduction using modified Woo filter form II.

The peak sidelobe level and integrated sidelobe level for Woo filter and for modified Woo filter of form-I and form- II for p4 code of length N = 1000 are shown in Table 4.1.

Table 4.1 PSL and ISL comparisons of various pulse compression techniques

Merit measures	Code length (N)	P4 code(dB)	Woo filter(dB)	Modified Woo filter form-I (dB)	Modified Woo filter form II. (dB)
PSL	1000	-36.36	-57.83	-88.57	-88.67
ISL	1000	-19.97	-30.1	-71.31	-72.60
PSL	2000	-39.37	-63.89	-97.65	-97.71
ISL	2000	-21.47	-33.1	-79.1	-80.0

The modified woo filter of form- I and form- II responses are shown in Fig (4.6) and (4.7). From the results it is observed that, PSL and ISL are reduced by significant amount in form-I and form-II. For length N=1000, around 32 dB of total PSL gain and 42 dB of total ISL gain is achieved by using modified Woo filter compared with Woo filter and 52 dB improvement of PSL and ISL over ordinary p4 code.

Peak sidelobe level and integrated sidelobe level are equal for both the forms. Form-I exhibits the uniform sidelobe level whereas in form-II this property was not achieved. Thus the modified model enhances the performance of pulse compression radar but at the sacrifice in range resolution.

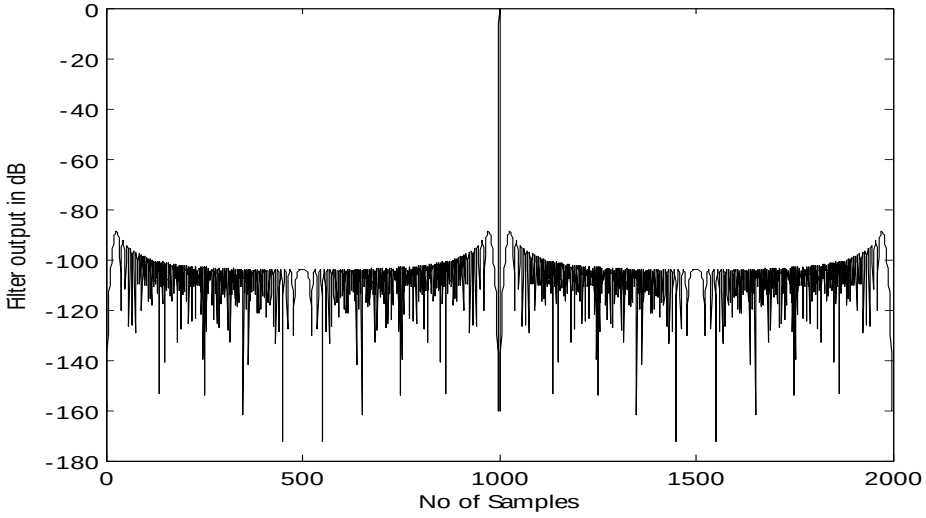

Figure 4.6 pulse compression output generated by modified Woo filter of form-I for p4 code of length 1000

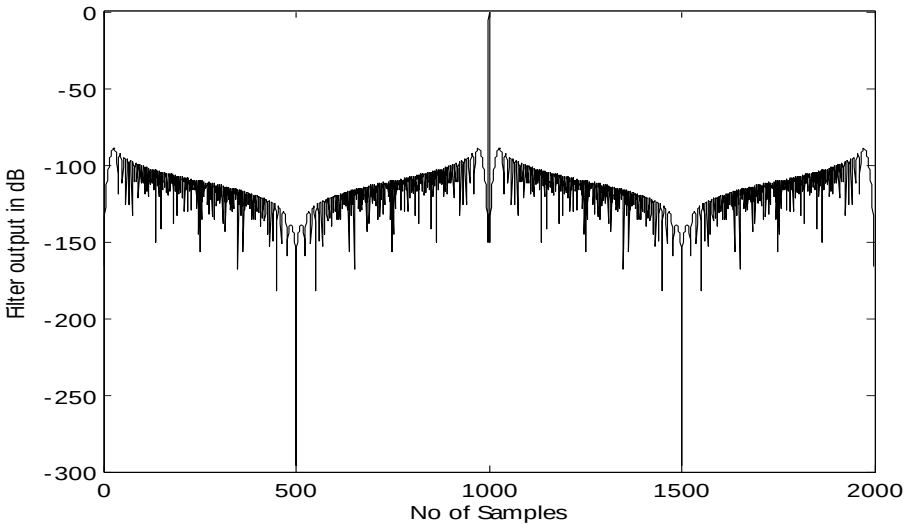

Figure 4.7 pulse compression output generated by modified Woo filter of form-I for p4 code of length 1000

4.4 Asymmetrical weighting receiver

In digital communication low autocorrelation levels are highly desirable. Conventional sidelobe reduction techniques which are discussed in chapter 2 have suffered from performance degradations in range resolutions and signal-to-noise ratio (SNR) gains. Asymmetrical weighting is a way to synthesize amplitude weight Correlators for polyphase codes. This technique generates sidelobes that are lower than those found in Barker codes. The sidelobe level is maintained uniformly flat over all time delays at the same time range resolution loss is prevented [4.1]. Unlike the Barker codes, the Asymmetrical weighting receiver is not limited by the code length, is easy to implement and incurs a minimal SNR loss. $P3$ and $P4$ codes are discrete polyphase codes which are directly derived from Linear FM signals[4.2]. Woo filter technique of sidelobe reduction makes use of the phase property of the P code to produce uniform sidelobe levels for. But the correlation of the Woo filter adds complexity in the receiver and degrades the range resolution by half and causes a 3 dB SNR loss. Hence still remains a demand for simple and efficient signal correlation techniques.

This Asymmetric weighting window which is explained this section for symmetric P codes that enables to suppress their PSLs below Barker code levels while other performance degradations such as mainlobe splitting and SNR are minimized. Woo filter which is constructed through a linear combination of two correlation filters and the amplitude components of this asymmetric window are discretely derived from the Woo filter. The array of these components is adjusted by removing redundant components to make it applicable on the symmetric P codes. This technique is free from the drawbacks of the conventional sidelobe reduction techniques and the advantageous property of having a uniform sidelobes is well preserved.

4.4.1 Weighting function approximation

A symmetric P code of length $N + 1$ elements is denoted as s-P. The n^{th} element of the s-P code is given as

$$s - P4(n) = exp\left(j\pi\left[\frac{n^2}{N} - n\right]\right) \tag{4.21}$$

Where $n = 0,1,2,\ldots\ldots,N$.The woo filter is directly derived from summation of two correlations filters in which the second one is time delayed version of the first filter. The q^{th} element of the woo filter array of length N is given as

$$Woo(q) = exp\left(-j\pi\left[\frac{q^2}{N} - q\right]\right) - exp\left(-j\pi\left[\frac{(q-1)^2}{N} - (q-1)\right]\right) \quad (4.22)$$

Where $1 \leq q \leq N$. From the above equations it is observed that woo filter is one bit less than s-P code and the woo filter gives rise mainlobe splitting and thus degrades the range resolution by half. From the nature of generating woo filter it is can be observed that the matched filter and woo filter have similar characteristics [4.9].

The phases variations of s-P code matched filter and woo filter are similar except at center intervals the variations rates are low. By increasing the length s-P code the phase variations of woo filter approaches the original matched filter [4.10]. From the above discussion of phase variations it is clear that matched filter and Woo filter and differ only in amplitude components. Equation (4.22) can be rearranged as

$$Woo(q) = 2jsin\left(\pi\left[\frac{-q+1/2}{N}\right]\right)exp\left(-j\pi\left[\frac{-q^2+q-1/2}{N}\right]\right)\exp(j\pi q) \quad (4.23)$$

From the phase and amplitude properties, if the magnitude of the Woo filter is taken as an amplitude weighting function to the original matched receiver, a good approximation to the Woo filter will be achieved in signal correlation. Since the Woo filter is shorter than the incoming signal by one bit, the newly constructed receiver can be adjusted to have a non-symmetrical phase variation. A new receiver filter is constructed by applying the magnitude of $|Woo(q)|$ to the matched filter as an amplitude window. Here the matched filter function is given as the conjugate of the original signal in (4.21).

The asymmetric receiver filter for the s- P code is synthesized by taking the magnitude q^{th} term of $sin\left(\pi\left[\frac{-q+1/2}{N}\right]\right)$ as weight factor on $exp\left(-j\pi\left[\frac{q^2}{N} - q\right]\right)$ term of the matched filter. Since the amplitude weighting array $|Woo(q)|$ is shorter than the original signal by one code element, the length of the matched filter should be shortened accordingly. This can be done by taking out the first or the last element of the matched filter and as a result the

symmetric property of the receiver filter is removed. For the s-P code array of length $N+1$ shown in (4.21), the corresponding amplitude weighted receiver is constructed by multiplying the weighting array $|Woo(q)|$ of length N *to* the conjugate sequence of either

$$\{s-P(0), s-P(1), \ldots\ldots\ldots\ldots\ldots..s-P(N-1)\}*$$

Or $$\{s-P(1), s-P(2), \ldots\ldots\ldots\ldots\ldots..s-P(N)\}*$$

In both cases, the receiver arrays are arranged in non-symmetrical ways while the phase characteristics of the original matched filters are maintained.

4.4.2 Correlation simulation

The correlation output produced by the asymmetric weight receiver is shown in Fig (4.7).

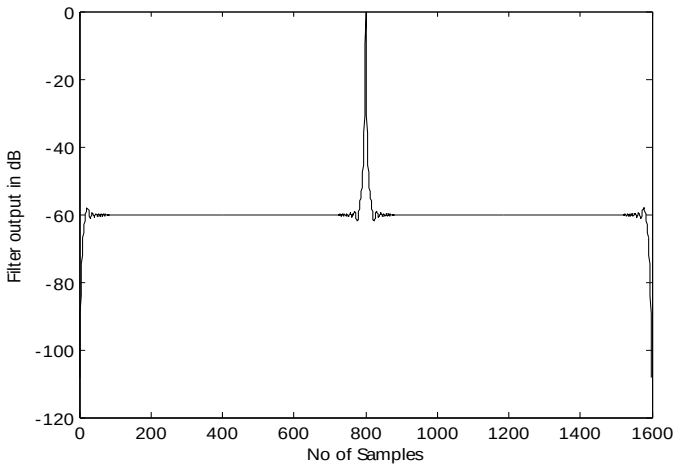

Figure 4.8 pulse compression output generated by Asymmetrical weighting receiver for p4 code of length 800

The Woo filter generates a uniform sidelobe of which is equivalent to the Barker code level but there exists mainlobe splitting. Here the Barker code level is defined as the reciprocal of the total code length or 1/N. Unlike the Woo filter case, the mainlobe peak generated by the asymmetric weight receiver has only one code element. This comparison is shown in Figure 4.8.

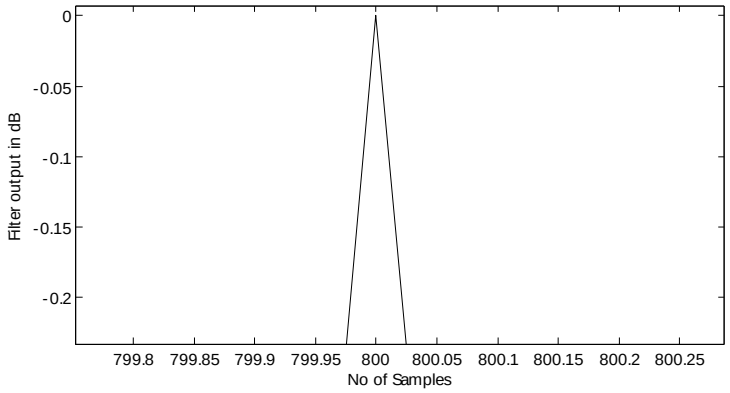

(a)

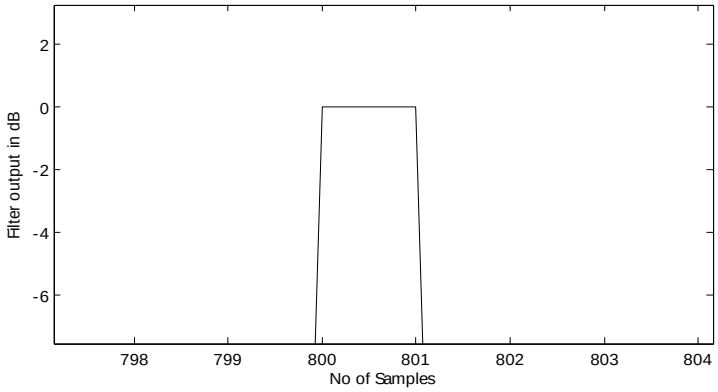

(b)

Figure 4.9 (a) Mainlobe generated by Asymmetrical weighting receiver (b) Mainlobe generated by Woo filter for p4 code of length 800

In the original Woo filter scheme, the mismatch between the incoming signal and the Woo filter results in two identical peaks at time delays of N -1 and N respectively. Consequently the range resolution is degraded by half. It is found that this technique consistently achieves a uniform sidelobe level of $20\ log10\ (1/N)\ -\ 2[dB]$ for an arbitrary code length N. The excellent performance of the technique is attributed to the unique sequences of the signals and receiver filters designated in equation (4.21)-(4.23). The use of sampling sequences other than (4.23) would fail to achieve the same result. Since the proposed Correlator is not perfectly matched to the incoming signal, there occurs a loss in SNR.

Table 4.2 shows the comparison of various performance measures of sidelobe reduction technique with Asymmetrical weighting discussed in this section for 800 element P code

Table 4.2 PSL and ISL comparisons of various pulse compression techniques

Techniques	Mainlobe broadening	Sidelobe[dB]	SNR loss[dB]	ISLR[dB]
No weighting	1	-17.6	0	-16.5
Hamming	1.36	-42.2	1.37	-15.9
Woo filter	2	-58	3	-29.1
Asymmetric weighting	1	-60	0.91	-19.7

4.3 Proposed Technique

In this technique combination of the input P4 signal and one-bit shifted version of the input signal is applied to amplitude weighting technique using different weighting techniques such as Hamming, Hanning, and Blackman etc... And then output is passed through matched filter. Here matched filter is used as the cross correlation between the amplitude weighted signal and the combined signal. This produces a high PSL and ISL than other techniques.

The implementation of this technique is shown in Figure 4.9

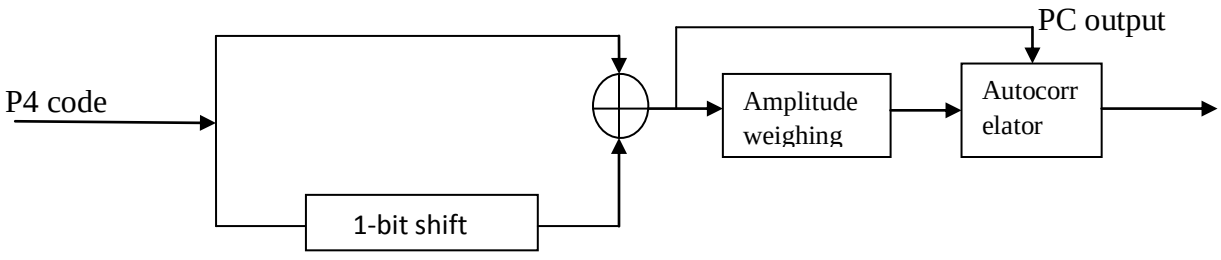

Figure 4.10 Schematic diagram of the proposed technique

Apart from producing better PSL and ISL than other technique it also eliminates the mainlobe boarding which is the major disadvantage in conventional sidelobes reduction techniques and Woo filter.

4.3.1 Simulation results of the proposed technique

In this section the correlation output of the proposed technique using different windows is shown and compared. Figure 4.10 shows the correlation outputs of Hamming, Hanning, Kaiser-Bessel and Blackman windows to the proposed technique.

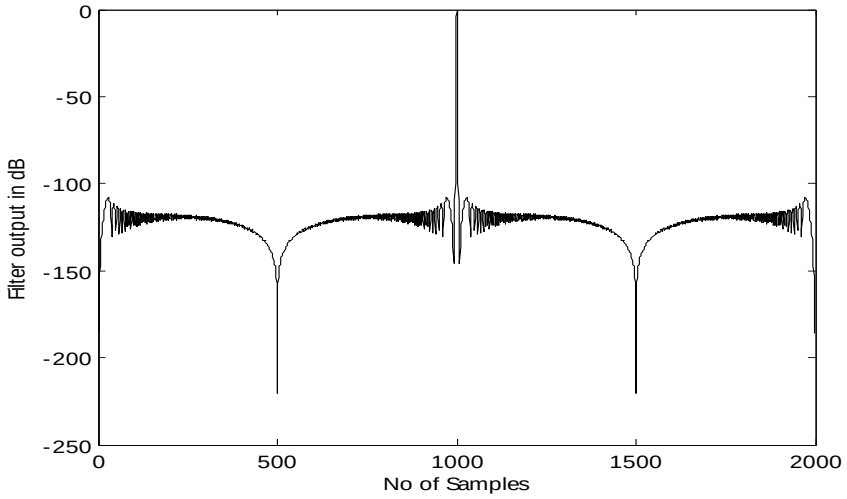

(a)

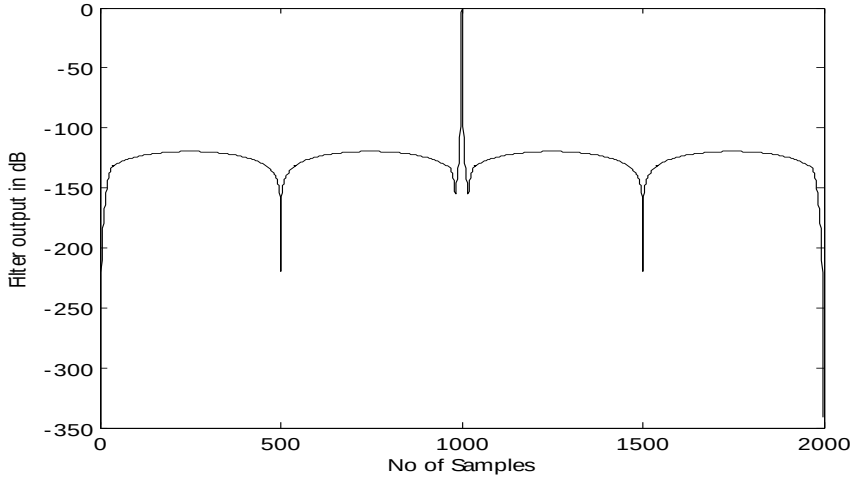

(b)

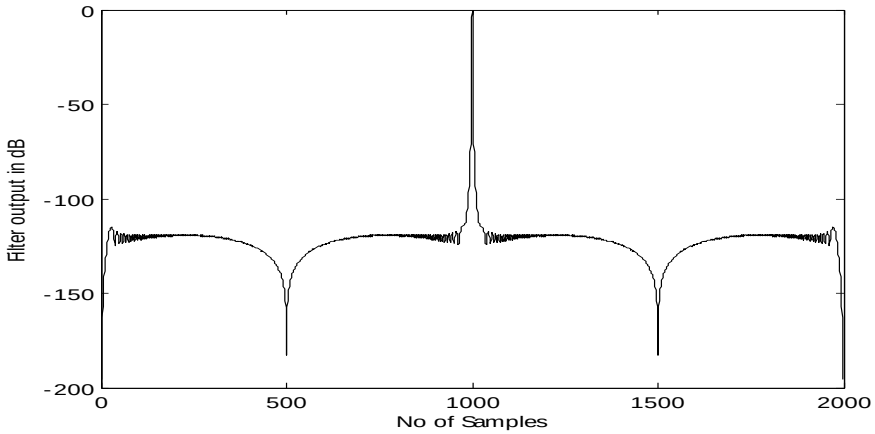

(c)

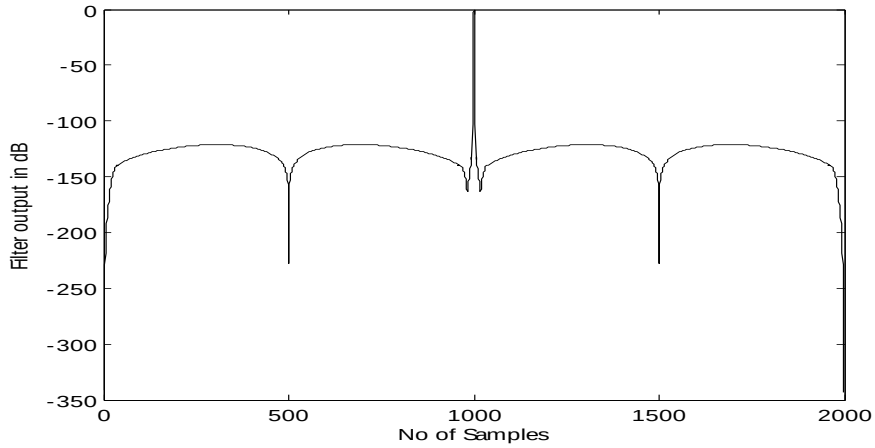

(d)

Figure 4.11 (a) Correlator output of the proposed technique (a) Hamming window (b) Hanning window (c) Kaiser-Bessel(β=5.44) (d) Blackman window for p4 code of length 1000

Thus from the above results the overall performance of the proposed technique produces better PSL than all other conventional sidelobe reduction techniques discussed in chapter2 and in the previous sections of this chapter. Apart from improvement of PSL mainlobe broadening is not present in any of the windows used. Amongst all the widows use the Blackman window produces highest PSL and ISL than all other windows. Comparison of the proposed technique with all techniques till now is shown in Table 4.2.

Table 4.3 PSL and ISL comparisons of various pulse compression techniques with the proposed technique

PC Techniques	PSL[dB]	ISL[dB]	SNR Loss [dB]
Hamming window	108.15	88.61	1.87
Hanning window	119.60	92.50	1.75
Kaiser-Bessel(β=5.44)	115.03	90.97	1.81
Asymmetrical weighting	-61	-30	0.912
Amplitude Weighting (Blackman)	-58.47	-33.21	2.37
Woo Filter	-59.83	-30.09	3
Woo Filter Form-2	-88.67	-70.06	3
New Technique (Blackman)	-121.2	-95.07	1.268

4.4. Summary

A detailed discussion and implementation of Woo filter and the extended versions of Woo filter which overcome the disadvantages present in Woo filter are also presented and comparison of PSL and ISL of all these techniques is also shown. A proposed technique is also discussed and compared with all other previous techniques.

Chapter 5

Conclusion and scope for future work

5.1 Conclusion

In this thesis, we have presented novel techniques for pulse radar detection. The concepts of pulse compression, phase coded pulse compression and different barker codes are studied. The major aspects for any pulse compression technique are signal to peak sidelobe ratio performance, noise performance and Doppler tolerance performance. Many techniques were employed to detect a radar pulse which includes classical amplitude, TSSWA, Woo filter and Asymmetrical Weighting. We proposed the new form of Woo filter for pulse radar detection which gave better results compared to other techniques. There is a scope of further improvement in all the aspects for most of the applications.

Chapter 2 gives a complete study of polyphase phase and why we go for polyphase codes form Biphase codes is explained. In this study, the performances of polyphase codes namely Frank, P1, P2, P3, P4 codes, how is codes are derived from frequency modulation, their autocorrelation properties, their phase values and their properties under Doppler shift conditions are discussed. A complete view of sidelobes and how these sidelobes are related is discussed.

Chapter 3 presents the sidelobe reduction techniques for polyphase codes. The Single TSSWA and double TSSWA outputs for P4 code are explained in detail and proved that this technique reduces the PSL value. In order to reduce the PSL values further, weighting techniques are employed. The Hamming and Kaiser Bessel windowing functions are studied and the performances of both the windows for P4 code are presented. The performance of Kaiser Bessel window depends on β parameter and proper choice of this parameter significantly reduces sidelobe level of compressed P4 signal. Also, this window has an additional advantage of being less sensitive to Doppler shift.

Chapter 4 discusses the Woo filter technique for sidelobe reduction and its advantages over all other techniques discussed in the previous chapters. The advanced versions of Woo filters such as Woo form-I and form-II are also discussed. Asymmetrical weighting technique which is used for symmetrical p- code is also discussed. A novel technique which we proposed is discussed and its advantages over original Woo filter and other conventional sidelobe techniques are explained.

5.2. Scope of Future Work

The work can be extended by improving PSL performance, SNR performance and Doppler shift interference by implementing the sidelobe cancellation technique which exactly cancels all the sidelobes as in the case of complementary code. There is a scope of designing a polyphase code which has lower sidelobes and is more Doppler tolerant than the codes discussed in the thesis by using the E_P4 code concept.

PUBLICATIONS

Vijay Ramya.K, A.k.Sahoo, G.Panda. "A New Pulse Compression Technique for Polyphase Codes in Radar Signals", *International Symposium on Devices MEMS Intelligent Systems Communications,* (ISSN 0975-8887) (ISBN 978-93-80747-80-2), pp.40-42, April-2011.

Post conference proceedings

Vijay Ramya.K, A.k.Sahoo, G.Panda. "A New Pulse Compression Technique for Polyphase Codes in Radar Signals", *International Journal of Computer Applications,* Submitted.

References

Chapter-1

[1.1] Merrill I. Skolnik, *Introduction to radar systems*, McGraw Hill Book Company Inc.,1962.

[1.2] Nadav Levanon, Eli Mozeson, "*Radar Signals*", 1.st Editon Wiley-Interscience, 2004.

[1.3] Carpentier, Michel H., "Evolution of Pulse Compression in the Radar Field," *Microwave Conference, 1979. 9th European*, vol., no., pp.45-53, 17-20 Sept. 1979

[1.4] R. L. Frank, "Polyphase Codes with Good Non periodic Correlation Properties", *IEEE Trans. on Information Theory*, vol. IT-9, pp. 43-45, Jan. 1963.

[1.5] B. L. Lewis, F. F. Kretschmer Jr., "A New Class of Polyphase Pulse Compression Codes and Techniques", IEEE *Trans. on Aerospace and Electronic Systems*, vol. AES-17, no. 3, pp. 364-372, May 1981.

[1.6] B. L. Lewis, F. F. Kretschmer Jr., "Linear Frequency Modulation Derived Polyphase Pulse Compression Codes", *IEEE Trans. on Aerospace and Electronic Systems*, vol. AES-18, no. 5, pp. 637-641, Sep. 1982.

[1.7] W.K.Lee, H.D.Griffiths and R.Benjamin. "Integrated sidelobe energy reduction technique using optimal polyphase codes", *Electrionic letter*, Vol.35, No.24, Nov.1999.

[1.8] W.K.Lee, H.D.Griffiths. "Pulse compression filters generating optimal uniform range sidelobe level". *Electronic Letter* 1999, Vol. 35.No.11.

[1.9] Woo-Kyung lee. "A Pair of asymmetrical weighting receivers and polyphase codes for efficient aperiodic correlations." *IEEE Communication Letters* Vol.10, No.5, May 2006.

Chapter-2

[2.1] Merrill I. Skolnik, *Introduction to radar systems*, McGraw Hill Book Company Inc.,1962.

[2.2] F.E. Nathanson, J. P. Reilly and M. N. Cohen, *"Radar Design Principles Signal Processing and the Environment"*, 2nd ed. New York: McGraw-Hill, 1999, chapt. 1 & 8.

[2.3] W. Siebert, "A Radar Detection Philosophy," *IRE Trans.*, vol.IT-2, no. 3, pp. 204-221, Sept. 1956.

[2.4] M.N.Cohen, J.M. Baden, and P. E. Cohen, "Biphase Codes with Minimum Peak Sidelobe," IEEE *International Radar Conf*, 1989, pp. 62-66.

[2.5] Nadav Levanon, Eli Mozeson, "Radar Signals", 1.st Editon Wiley-Interscience, 2004.

[2.6] M.G. Parker, K.G. Paterson & C. Tellambura, "Golay Complementary Sequences", in Wiley Encyclopedia of Telecommunications, John G. Proakis, ed., Wiley, 2003

[2.7] S. Searle, S. Howard, "A Novel Polyphase Code for Sidelobe Suppression", Invited Paper, *IEEE Trans. On Waveform Diversity and Design*, 2007.

[2.8] Talal Darwich, "*High Resolution Detection Systems using Low Sidelobe Pulse Compression Techniques*", Ph.D. Thesis, University of Louisiana, 2007.

[2.9] R. L. Frank, "Polyphase Codes with Good Nonperiodic Correlation Properties", *IEEE Trans. on Information Theory*, vol. IT-9, pp. 43-45, Jan. 1963

[2.10] B. L. Lewis, F. F. Kretschmer Jr., "A New Class of Polyphase Pulse Compression Codes and Techniques", IEEE *Trans. on Aerospace and Electronic Systems*, vol. AES-17, no. 3, pp. 364-372, May 1981

[2.11] B. L. Lewis, F. F. Kretschmer Jr., "Linear Frequency Modulation Derived Polyphase Pulse Compression Codes*", IEEE Trans. on Aerospace and Electronic Systems*, vol. AES-18, no. 5, pp. 637-641, Sep. 1982

[2.12] B. L. Lewis, "Range-Time-Sidelobe Reduction Technique for FM-Derived Polyphase PC Codes*", IEEE Trans. on Aerospace and Electronic Systems*, vol. AES-29, no. 3, pp. 834-840, July 1993

Chapter-3

[3.1] B. L. Lewis, F. F. Kretschmer Jr., "A New Class of Polyphase Pulse Compression Codes and Techniques", IEEE *Trans. on Aerospace and Electronic Systems*, vol. AES-17, no. 3, pp. 364-372, May 1981

[3.2] B. L. Lewis, "Range-Time-Sidelobe Reduction Technique for FM-Derived Polyphase PC Codes*", IEEE Trans. on Aerospace and Electronic Systems*, vol. AES-29, no. 3, pp. 834-840, July 1993

[3.3] Woo-Kyung lee, Hugh D.Griffiths. “A new pulse compression Techniques Generating Optimal uniform Range sidelobe and reducing integrated sidelobe level.” *IEEE International Radar Conference* 2000

[3.4] F. F. Kretschmer Jr., L. R. Welch, “Sidelobe Reduction Techniques for Polyphase Pulse Compression Codes”, *IEEE International Radar Conference*, pp. 416-421, May 2000.

[3.5] M. Luszczyk, D. Mucha, "Kaiser-Bessel window weighting function for polyphase pulse compression code," *Microwaves, Radar and Wireless Communications, 2008. MIKON 2008. 17th International Conference on* , vol., no., pp.1-4, 19-21 May 2008.

[3.6] Oppenheim, A.V., and R.W. Schafer, *“Discrete-Time Signal Processing*”, Prentice-Hall, 1989, pp. 447-448.

[3.7] Frank F. Kretschmer and Laurence R. Welch, *“*Sidelobe reduction techniques for polyphase pulse compression codes” *IEEE International Radar Conference* Pp.416-421.

[3.8] Kaiser, J.F., "Nonrecursive Digital Filter Design Using the I0- sinh Window Function," *Proc. 1974 IEEE on Symp. Circuits and Systems*, (April 1974), pp.20-23.

Chapter-4

[4.1] B. L. Lewis, “Range-Time-Sidelobe Reduction Technique for FM-Derived Polyphase PC Codes*”, IEEE Trans. on Aerospace and Electronic Systems*, vol. AES-29, no. 3, pp. 834-840, July 1993

[4.2] Woo-Kyung lee, Hugh D.Griffiths. “A new pulse compression Techniques Generating Optimal uniform Range sidelobe and reducing integrated sidelobe level.” *IEEE International Radar Conference* 2000.

[4.3] W.K.Lee, H.D.Griffiths and R.Benjamin. Integrated sidelobe energy reduction technique using optimal polyphase codes .*Electronic Letter* 1999, Vol. 35. No.24, pp. 2090-2091.

[4.4] Lewis, B.L., and Krestschmer. “Linear frequency modulation derived polyphase pulse compression codes.” *IEEE Trans Aerospace Electron Syst* 1982; AES-18, No. 5, pp.637-641.

[4.5] Shamsolan Salemain and Hamid Keivandi and Omed Manhdiyan. “Comparison of Radar Signal Compression Techniques.” 2005 *IEEE International Symposium on Microwave, Antenna, Propagation and EMC Technologies for Wireless Communication Proceedings*, pp. 1076-1079.

[4.6] W.K.Lee, H.D.Griffiths. “Pulse compression filters generating optimal uniform range sidelobe level”. *Electronic Letter* 1999, Vol. 35.No.11, pp. 873-875.

[4.7] Woo-Kyung lee, Hugh D.Griffiths. “A new pulse compression Techniques Generating optimal uniform Range sidelobe and reducing integrated sidelobe level.” *IEEE International Radar Conference* 2000, pp. 441-446.

[4.8] Uttara M.Kumaria, K.Rajearakeswari, Murali K.Krishna. “Low sidelobe Pattern using Woo filter”. *Concept .Int.J.Electron.Commun.(AEU)* 59(2005), pp. 499-501

[4.9] Woo-Kyung lee. “A Pair of asymmetrical weighting receivers and polyphase codes for Efficient aperiodic correlations.” *IEEE Communication Letters* Vol.10, No.5, May 2006, pp. 387-389.

[4.10] W.K.Lee, H.D.Griffiths, “Development of modified polyphase P codes with optimum Sidelobe characteristics.” IEEE *Proc.Radar, Sonar Navig*, Vol. 151, pp. 210-220, Aug. 2004.